

**USING TISSUE CULTURE TO MODEL EARLY EVENTS IN *FRANCISELLA*  
*TULARENSIS* PATHOGENESIS**

by

**Jennifer Burwinkel**

BS Biology, Montreat College, 2015

Submitted to the Graduate Faculty of  
the Department of Infectious Diseases and Microbiology  
Graduate School of Public Health in partial fulfillment  
of the requirements for the degree of  
Master of Science

University of Pittsburgh

2018

UNIVERSITY OF PITTSBURGH  
GRADUATE SCHOOL OF PUBLIC HEALTH

This thesis was presented

by

Jennifer Burwinkel

It was defended on

April 6, 2018

and approved by

**Thesis Director:**

Douglas S Reed, PhD  
Associate Professor  
Department of Immunology  
School of Medicine  
University of Pittsburgh

**Committee Member:**

Joshua T Mattila, PhD  
Assistant Professor  
Infectious Diseases and Microbiology  
Graduate School of Public Health  
University of Pittsburgh

**Committee Member:**

Robbie B Mailliard, PhD  
Assistant Professor  
Infectious Diseases and Microbiology  
Graduate School of Public Health  
University of Pittsburgh

Copyright © by Jennifer Burwinkel

2018

**USING TISSUE CULTURE TO MODEL EARLY EVENTS IN *FRANCISELLA*  
*TULARENSIS* PATHOGENESIS**

Jennifer Burwinkel, MS

University of Pittsburgh, 2018

**ABSTRACT**

*Francisella tularensis* (*Ft*) is a highly infectious bacterium that causes tularemia, which manifests in multiple presentations such as ulceroglandular, pneumonic, or typhoidal forms. Pneumonic tularemia, a more severe manifestation, can result from inhalation of as few as 10 colony forming units of *Ft*. The low infectious dose, its potential for aerosolization, and severity of disease has resulted in *Ft* classification as a Select Agent by the CDC for bioweapon potential. The severe clinical and financial burden a bioweapon attack utilizing *Ft* would impose on the U.S. makes development of therapeutics and vaccines an important contribution to protecting public health. Determination of vaccine targets requires knowledge of the early pathogenesis of *Ft* in the lungs. *Ft* infects a wide variety of cells, including lung macrophages and lung epithelial cells, likely involved in initial infection from aerosol; few have compared the permissivity of infection between these cell types to infection by *Ft*. We utilized an *in vitro* infection assay with murine macrophages (J774) and human alveolar epithelial cells (A549), and developed an *ex vivo* infection assay for 3D-cultured human primary bronchial epithelium (HBE), intended to mimic lung architecture. Early cellular events within SCHU S4 infected rabbit tissue, a model which exhibits clinical disease similar to humans, was assessed for cellular infiltration, changes in lung architecture, and apoptosis. I found that different strains of *Ft* (SCHU S4, LVS, and U112), grow at similar rates in A549 as J774 after initial infection. Moreover, I have

demonstrated that *Ft* can infect HBE in the 3D culture system. These data suggest that it takes *Ft* longer to infect the HBE cells than the A549 or J774 cells. This is the first infection assay performed within a 3D HBE culture, to our knowledge. Over the course of the first five days post-exposure there is an increasing amount of inflammation, hemorrhaging and apoptosis in rabbit lung. When taken altogether, these data suggest lung epithelial cells have an underappreciated role in *Ft* early pathogenesis and dissemination.

## TABLE OF CONTENTS

<b>PREFACE.....</b>	<b>XII</b>
<b>1.0 INTRODUCTION.....</b>	<b>1</b>
<b>1.1 TULAREMIA .....</b>	<b>1</b>
<b>1.2 HUMAN INFECTION .....</b>	<b>1</b>
<b>1.3 ANIMAL MODELS .....</b>	<b>3</b>
<b>1.3.1 Rabbits.....</b>	<b>3</b>
<b>1.3.2 Mice.....</b>	<b>4</b>
<b>1.4 FRANCISELLA TULARENSIS .....</b>	<b>4</b>
<b>1.4.1 U112 .....</b>	<b>5</b>
<b>1.4.2 Live Vaccine Strain .....</b>	<b>5</b>
<b>1.4.3 SCHU S4.....</b>	<b>6</b>
<b>1.5 CELL TYPES.....</b>	<b>6</b>
<b>1.5.1 Murine Macrophages .....</b>	<b>6</b>
<b>1.5.2 Human Alveolar Epithelium.....</b>	<b>7</b>
<b>1.5.3 Human Primary Lung Epithelium.....</b>	<b>7</b>
<b>1.6 CELL DEATH .....</b>	<b>8</b>
<b>1.6.1 Types of cell death .....</b>	<b>8</b>
<b>1.6.2 Apoptosis .....</b>	<b>9</b>

1.6.3	Pyroptosis .....	9
1.7	PUBLIC HEALTH SIGNIFICANCE.....	10
2.0	SPECIFIC AIMS.....	11
2.1	AIM 1: TO USE AN IN VITRO MODEL OF INFECTION WITH LVS AND SCHU S4 IN HUMAN ALVEOLAR EPITHELIUM AND HUMAN PRIMARY LUNG EPITHELIUM.....	11
2.2	AIM 2: PATHOGENESIS OF SCHU S4 IN RABBIT LUNG TISSUE.....	12
3.0	MATERIALS AND METHODS .....	13
3.1	BIOSAFETY .....	13
3.2	RABBITS.....	13
3.3	CELL CULTURE.....	14
3.4	BACTERIA .....	14
3.5	INFECTION ASSAY.....	15
3.6	HBE INFECTION ASSAY .....	16
3.7	CASPASE-3 FLUORESCENT ASSAY IN CELL CULTURES.....	17
3.8	CASPASE-3 FLUORESCENT ASSAY IN TISSUES.....	18
3.9	CASPASE-1 FLUORESCENT ASSAY IN CELL CULTURES.....	18
3.10	CASPASE-1 FLUORESCENT ASSAY IN TISSUES.....	19
3.11	HEMATOXYLIN AND EOSIN STAINING .....	20
3.12	TUNEL ASSAY .....	20
3.13	SLIDE CUTTING.....	22
3.14	LUNG DIGEST .....	23
4.0	IN VITRO MODEL OF INFECTION.....	24

4.1.1	Initial Infection Assays.....	24
4.1.2	Lung Epithelial Cell Infection .....	28
4.1.3	Human Primary Lung Infection .....	32
4.2	PATHOGENESIS IN RABBIT LUNGS .....	41
4.2.1	Caspase Assays.....	43
4.2.2	Lung Slides .....	44
5.0	DISCUSSION .....	51
	BIBLIOGRAPHY.....	57



## LIST OF TABLES

Table 1. J774 and A549 Infection.....	25
Table 2. J774 Infection Assay.....	26
Table 3. A549 Infection Assay 1. ....	27
Table 4. A549 Infection Assay 2. ....	29
Table 5. A549 Infection Assay 3. ....	30
Table 6. HBE Infection Assay 1. ....	33
Table 7. HBE Assay 2 Plate Setup.....	33
Table 8. HBE Infection Assay 2. ....	34
Table 9. HBE Infection Assay 3. ....	34
Table 10. HBE Infection Assay 4. ....	35
Table 11. HBE Infection Assay 5. ....	37
Table 12. HBE Infection Assay 6. ....	38
Table 13. HBE Infection Assay 7. ....	39
Table 14. HBE Infection Assay 8. ....	40

## LIST OF FIGURES

Figure 1. J774 Infection Assay. ....	26
Figure 2. A549 Infection Assay 1. ....	28
Figure 3. A549 Infection Assay 2. ....	29
Figure 4. A549 Infection Assay 3. ....	31
Figure 5. A549 Caspase-1 and Caspase-3. ....	31
Figure 6. LVS and SCHU S4 colony counts in HBE cell lysate 24 hours post-infection. ....	35
Figure 7. HBE Infection Assay 4. ....	36
Figure 8. HBE Infection Assay 5. ....	37
Figure 9. HBE Infection Assay 6. ....	38
Figure 10. HBE Infection Assay 7. ....	40
Figure 11. HBE Infection Assay 8. ....	41
Figure 12. <i>Francisella tularensis</i> in Rabbit Lung Tissue. ....	43
Figure 13. Rabbit Caspase Staining. ....	44
Figure 14. Inflammation in the lower left lung of rabbits sacrificed one to three days post-exposure to SCHU-S4. ....	45
Figure 15. DNA fragmentation in the lower left lung of rabbits sacrificed one to three days post-exposure to SCHU-S4. ....	46

Figure 16. Inflammation in the upper right lung rabbits sacrificed one to three days post-exposure to SCHU-S4..... 47

Figure 17. DNA fragmentation in upper right lung of rabbits sacrificed one to three days post-exposure to SCHU-S4..... 48

Figure 18. Inflammation in the lung of rabbits sacrificed four and five days post-exposure to SCHU S4..... 49

Figure 19. DNA fragmentation in lung tissue from rabbits sacrificed four and five days post-exposure to SCHU S4. .... 50

## PREFACE

I would like to thank my mentor, Dr. Doug Reed. He was unsure if he could take on two additional students and I am grateful he decided to take me on anyways. His experience with the infection assay was extremely helpful. Also, his guidance helped me expand my laboratory skills and critical thinking, especially when problem solving.

Also, I would like to thank everyone in the Reed Lab: Katie Willett, Megan Beary, Jennifer Bowling and Henry Ma. Their willingness to answer all my questions is greatly appreciated. Also, their willingness to help any day at any time is appreciated. I cannot list everything I am thankful for.

I would like to thank Dr. Amy Hartman's lab for providing the A549 cells for me to use. Also, I would like to thank Dr. Mike Myerburg's Lab for providing me with the human primary bronchial cell cultures. I would especially like to thank Anastasia Jacko for meeting with me every time I needed cells. Also, I am grateful for their guidance when I was having issues with the HBE infection assays.

Finally, I would like to thank Tim Oury's lab for allowing me to use their microtome and answering my questions related to slide cutting. Also, I would like to thank Dr. Josh Mattila for helping me image my lower left lung slides.

## **1.0 INTRODUCTION**

### **1.1 TULAREMIA**

Tularemia is the disease caused by *Francisella tularensis*. Humans can be infected by multiple routes including a bite by an arthropod vector, contact with an infected animal or carcass, ingestion of contaminated water or food and inhalation of the organism. It is not transmitted from human -to -human. *Francisella* is endemic in several areas of the world. The outbreaks of tularemia do not seem to follow any specific pattern from year-to-year. It is typically a seasonal disease. The incidence is highest from late spring to early fall [1]. There was an outbreak in the Rostov-on-Don region of the Soviet Union during 1941-42, in which 67,000 cases were reported. The United States has had several outbreaks; however, only 14,000 cases were reported from 1920 to 1945. The number of reported cases worldwide has decreased since the 1950s. Between 1990 and 2000, the United States only had 1,400 reported cases [1].

### **1.2 HUMAN INFECTION**

As mentioned previously, humans can be infected by *Francisella tularensis* through multiple routes. Each route shows different clinical presentation. The disease course is similar to other infectious diseases, which can make diagnosis difficult. The incubation period can range

from 1-21 days; however, the typical incubation period is 3-5 days. The disease onset is very rapid. It includes fever, chills, fatigue, body aches and headache. The bacteria replicate rapidly at the beginning of infection. The immunologic response is very important in controlling the disease. Cell-mediated responses are more important than antibody-mediated responses because the antibodies do not play an important role in preventing the disease or lessening severity. However, antibodies can be good for diagnosis [1].

The strains from the subspecies *tularensis* (Type A) can cause significant mortality if left untreated. There are occasional cases of rhabdomyolysis and septic shock associated with disease caused by the subspecies *tularensis*. With the advent of effective antibiotics, the mortality rate is less than two percent. However, when the disease is untreated, the mortality rate can be as high as thirty to sixty percent. The symptoms of disease caused by this subspecies include: high fever, progressive weakness, malaise, anorexia, weight loss, dry cough, sore throat, substernal pain and occasionally gastrointestinal symptoms [1].

The subspecies *holarctica* (Type B) is typically transmitted via infected water, it can also be transmitted the same ways as Type A strains. The predominant symptom associated with Type B infection is fever. There have been more cases of tularemia caused by Type B strains than Type A strains worldwide. Type B strains are not as virulent as Type A strains, but can cause substantial morbidity and mortality. The disease caused by the subspecies *mediasiatica* is similar to that caused by the subspecies *holarctica* and is rarely reported in humans [1].

The subspecies *novicida* is avirulent in humans. Occasionally, it will cause disease in immunocompromised individuals. It has been reported in four individuals in the United States. Three of the four cases were in immunocompromised individuals. It has caused disease in several individuals in Canada, Australia and Spain too [1].

Respiratory illness is caused by inhalation of aerosolized *F. tularensis*. The respiratory illness may present initially as pneumonia. The respiratory disease varies greatly between Type A and Type B strains. The symptoms associated with Type A caused disease are chills, high fever, dyspnea, dry or productive cough, pharyngitis, chest pain, headache, profuse sweating, drowsiness and weakness. The symptoms can be severe and resemble typhoid fever. The disease caused by Type B strains varies. Some outbreaks have a small percentage of cases with pneumonia like symptoms. Other outbreaks have a high percentage of pulmonary changes [1].

### **1.3 ANIMAL MODELS**

*Francisella* infects a wide range of mammals. Hares, prairie dogs, voles, squirrels, beavers, mice and many others can all be infected with *Francisella*. The spread of *Francisella* in the Soviet Union was thought to have been caused by voles and mice. Also, several people have become infected after running a rabbit or rabbit den over with the lawn mower. Therefore, there is a broad range of animal models available. However, tularemia in many animal species has not been characterized [1]; therefore, it is difficult to find an appropriate animal model [2]. Several animals used in tularemia research are guinea-pigs, rabbits, rats, mice and monkeys.

#### **1.3.1 Rabbits**

The clinical presentation of *Francisella* infection in rabbits is like humans. The rabbits can develop a fever, lose weight, experience lethargy, decreased appetite and occasional diarrhea. *Francisella* can infect many organs in a rabbit's body. For example, lung, spleen, liver,

kidney, intestine, and lymph node involvement has been found during *Francisella* infection. These organs have been involved in the human infection as well [2].

### 1.3.2 Mice

Mice have been used extensively in tularemia research. Mice vary from humans in susceptibility to different strains of *Francisella*. They are susceptible to both *tularensis* and *holarctica* subspecies of *Francisella*. There is initially a reduced inflammatory response to infection with either strain [1]. Mice infected with SCHU S4 experience ruffled fur, lethargy, anorexia and hunching with infected via aerosol and intranasally. Like humans, mice can have lung, spleen and liver involvement [2].

## 1.4 FRANCISELLA TULARENSIS

*Francisella tularensis* is a gram-negative facultative intracellular bacterium that causes tularemia. *Francisella* is in a group of bacteria with *Listeria*, *Legionella* and *Rickettsia* [1]. *F. tularensis* can infect a broad range of hosts, including humans. The disease varies based on route of infection and bacterial subtype [3].

The intracellular life cycle for *Francisella tularensis* has been studied in murine macrophages. First, *F. tularensis* is phagocytosed and remains in the *Francisella*-containing phagosome. *F. tularensis* is released into the macrophage cytosol after the phagosome membrane is disrupted. There is extensive replication in the cytosol. Eventually the bacteria are released when the cells undergo cell death. The cycle then repeats itself [4].



### 1.4.1 U112

There are two avirulent subspecies of *F. tularensis* as well: *mediasiatica* and *novicida* [5]. Infection with *F. tularensis* subsp. *novicida* is extremely rare in humans. Strain U112, which is used in this study, is in the subspecies *novicida*. *F. novicida* can be transmitted through ingestion of infected water. Unlike *F. tularensis* there are no known animal or arthropod hosts for *F. novicida* [6], but U112 is able to enter and replicate within amoebas [7].

### 1.4.2 Live Vaccine Strain

An attenuated strain of *F. tularensis holarctica*, the Live Vaccine Strain (LVS), is used in this study. The LVS strain is originally derived from a strain used as a vaccine in the Soviet Union. During World War II, there was an outbreak of tularemia among the Soviet soldiers [8]. There were 67,000 cases of tularemia reported in 1941-42 in the Soviet Union [1]. LVS was developed to help reduce the number of tularemia cases among the soldiers. There was a reduction of tularemia cases; however, sanitation improvements could also explain the reduction. In 1956, the Soviet Union gave the strain to investigators at Fort Detrick. The investigators further attenuated the pathogen to give to at-risk personnel. The reasons for LVS attenuation remain unknown because the parent strain is unknown. Therefore, the LVS strain cannot be used as a vaccine because of the potential to revert [8]. LVS is the most commonly studied strain of *F. tularensis* because it mimics many of the features of virulent *F. tularensis* in culture but can be safely work with at BSL-2.

### **1.4.3 SCHU S4**

The virulent strain of *F. tularensis* subsp. *tularensis* used in this study is SCHU S4. SCHU S4 was originally isolated from a patient in Ohio in 1941 [2]. SCHU S4 is the prototype strain of virulent *F. tularensis* that is studied in laboratories.

## **1.5 CELL TYPES**

It is widely believed that the major targets of *F. tularensis* are macrophages and dendritic cells [3]. However, *F. tularensis* can infect a wide variety of eukaryotic cell types including hepatocytes, osteoblasts, epithelial cells, erythrocytes, and even fresh water amoeba [2, 5, 9, 10]. Considering that the respiratory infectious dose is 15 CFU in humans, the bacterium's initial interactions in the respiratory tract are likely to be with epithelial cells. Therefore, it seems reasonable that *F. tularensis* infection of lung epithelial cells in early pathogenesis of this pathogen in order to develop a vaccine to prevent infections.

### **1.5.1 Murine Macrophages**

The J774 cell line was derived from a BALB/cN female mouse with reticulum cell sarcoma [11]. This cell line is a macrophage-like cell line [12]. J774 cells have been used to determine the best lysing solution when working with *Francisella* [13], the cytokine and chemokine patterns during *Francisella* infection [14], and the factors involved in the *Francisella* Type IV secretion system [15].

### **1.5.2 Human Alveolar Epithelium**

The A549 cell line was derived from a 58-year-old male with carcinoma [16]. These cells are alveolar type II epithelial cells [12]. A549 cells have been used to study *Francisella* entry via micropinocytosis [17], immune suppression [17], differences in 2D and 3D cell culture responses to infection [18], ability of *Francisella* to infect human lung epithelium [12] and adherence to nonphagocytic cells [19].

### **1.5.3 Human Primary Lung Epithelium**

Most epithelial cell research *in vitro* is done with 2D monolayer cell cultures. However, these cell cultures are very different from the structure of the cells in the lungs. Cells cultured in a monolayer on hard plastic lose certain phenotypic characteristics. This results in changes in their function, biochemistry and morphology [18]. More recently 3D cell cultures have been used to more accurately model the lung epithelium. Cells in 3D cultures have cilia, apical-basal polarity, and produce mucus unlike 2D monolayers.

For example, A549 cells grown in a flask do not display the same phenotypic characteristics as A549 cells grown using rotary wall vessel (RWV) bioreactors. The RWV bioreactor rotates the vessel horizontally. The cells are in a constant free-fall within the culture. This allows the cells to attach to one another creating a tissue-like phenotype. A549 cells grown in the RWV suspension culture have tight junctions and adherens junctions. A549 cells in 2D culture have type IV collagen localization in the nucleus, but 3D cultured have basolateral surface localization. There are also differences in the presence of laminin. Collagen and laminin are important in adhesion of the cells to the extracellular matrix. This suggests that there is

polarization of the A549 cells in RWV cultures. A549 monolayer cultures produce very low levels of respiratory mucins and the production of the mucins is intracellularly. The 3D cultures of A549 cells show higher levels of mucin production at the apical side of the culture, indicating proper mucin location for mucous production [20]. RWV cultured A549 cells seem to be more resistant to *F. tularensis* infection suggesting that 3D cultures better predict what was going on *in vivo* during infection.

By using a 3D culture, the ability of *F. tularensis* to infect human primary epithelial cells can be evaluated. Therefore, the use of the 3D cultures may give us a better idea of what is going on in the lung epithelium during infection with *F. tularensis*.

## **1.6 CELL DEATH**

### **1.6.1 Types of cell death**

There are three known types of cell death: necrosis, apoptosis and pyroptosis. For apoptosis, activated proteases and ATP is required. Cells undergoing apoptosis maintain cell membrane integrity until the late stages of the process. During necrosis, cell membrane damage occurs either directly or indirectly. Cells undergo energy depletion, swell and leak their cytoplasmic contents. Pyroptosis is a caspase-1 dependent form of necrosis. Apoptosis does not elicit a high inflammatory response; whereas, pyroptosis and necrosis do [21].

### **1.6.2 Apoptosis**

In apoptosis, cells maintain membrane integrity up until they are engulfed by the phagocytes. This type of cell death does not cause an immunologic response. Therefore, a pathogen could be causing cell death without triggering an inflammatory response. Although, the pathogen may activate the phagocytes that engulf the dead cells [22]. Apoptosis has initiator and effector caspases. The initiator caspases include caspase-2, 8, and 9. The effector caspases are caspase-3, 6, and 7.

There are two apoptosis pathways: extrinsic pathway and intrinsic pathway. The extrinsic pathway is activated by extracellular ligands and death receptors. This pathway uses caspases 3, 6, 7, 8, and 10. During the intrinsic apoptosis signaling, cytochrome c is released from the mitochondria. It activates the formation of the apoptosome which recruits pro-caspase-9. Pro-caspase-9 gathers by the apoptosome, which activate it. The apoptosome cleaves pro-caspase-3 into caspase 3. Caspase-3 cleaves ICAD into CAD, which ultimately cleave the DNA in the nucleus [23]. Cell shrinkage and blebbing are characteristics of cells undergoing apoptosis.

### **1.6.3 Pyroptosis**

Two different types of programmed cell death have been well described, which include those that fall under the category of either apoptosis or pyroptosis. Pyroptosis is commonly caused by infections with pathogens. This type of cell death does have an inflammatory response. IL-1 $\alpha$ , IL-1 $\beta$ , and IL-18 are commonly released causing the inflammatory response [22]. Pyroptosis is inflammasome-dependent. There are several caspases involved in this process: caspase-1 and mouse caspase-11.

Pyroptosis can be triggered by cell damage. Bacterial toxins or activation of the P2X7 receptor are two examples of cell damage known to activate pyroptosis. After activation, potassium is released from the cell. NLRP3 is activated when the chaperones dissociate due to efflux of potassium. Several NLRP3 domains interact with the adaptor protein ASC. The CARD domains of ASC aggregate causing the CARD domains of caspase-1 to aggregate. The caspase-1 is then cleaved into its' active form. The active caspase-1 then cleaves immature pro-inflammatory cytokines including IL-18 and IL-1 $\beta$ . Alternatively, there is a caspase-1 independent inflammasome pathway. Caspase-11 detects intracellular lipopolysaccharide [23]. In pyroptosis there is an influx of fluid, causing the cell to swell and ultimately lyse [22].

## **1.7 PUBLIC HEALTH SIGNIFICANCE**

*Francisella tularensis* is an ideal biological warfare agent for many reasons. Its' low infectious dose and aerosol delivery make it an ideal agent. SCHU S4 was weaponized in the past by the Soviet Union and the United States [8]. While tularemia is treatable, it is important to have a vaccine for it. Since there is not a vaccine, research on how the virulent strain infects versus the less virulent strains is very important. It could provide information on how to create a vaccine against the agent. Therefore, it would be easier to prevent natural outbreaks as well as to protect against its' use in biological warfare.

## **2.0 SPECIFIC AIMS**

Currently, the early pathogenesis of *Francisella* in lung epithelial cells is unknown. This project focuses on the ability of *Francisella* to infect and replicate within lung epithelial cells and cell death and inflammation in rabbit lung tissues. This will be accomplished by comparing results from in vitro work with transformed cell lines, human primary lung cells and tissue samples from infected rabbits.

### **2.1 AIM 1: TO USE AN IN VITRO MODEL OF INFECTION WITH LVS AND SCHUS4 IN HUMAN ALVEOLAR EPITHELIUM AND HUMAN PRIMARY LUNG EPITHELIUM**

The goal of this aim is to determine if *Francisella tularensis* can infect human alveolar epithelium (A549) and human primary lung epithelium (HBE) and establish infection assay protocols. This will be accomplished by:

- a. Performing infection assays to determine if *F. tularensis* can infect human primary lung epithelium
- b. Determining growth rates of *F. tularensis* in both A549 and primary lung epithelium

- c. Establish an infection assay protocol for the human primary lung epithelium

## **2.2 AIM 2: PATHOGENESIS OF SCHU S4 IN RABBIT LUNG TISSUE**

The goal of this aim is to determine whether the animal model correlates with the *in vitro* and *ex vivo* models. This correlation will be assessed by:

- a. Determining the presence and concentration of *F. tularensis* in the tissue samples
- b. Determining whether cell death is occurring in the tissue samples
- c. Determining if inflammation and hemorrhaging are increasing each day post-exposure in the tissue samples



### **3.0 MATERIALS AND METHODS**

#### **3.1 BIOSAFETY**

All work with the SCHU S4 strain of *Francisella* was done in BSL-3+ laboratories. Work with this agent included wearing a disposable gown, rubber work boots, double gloves and a powered air purifying respirator (PAPR). All materials used during work with agent were disinfected with vesphene, double bagged and autoclaved. Work with U112 and LVS strains of bacteria was done in BSL3+ as well as BSL2 laboratories. The same procedures for BSL3+ as above were used. The BSL2 procedures include working in a Class II Biosafety cabinet, with gloves and splashguard gown. Bleach is used as a disinfectant in the BSL2 laboratories.

#### **3.2 RABBITS**

Female New Zealand White rabbits were housed in the BSL-3 laboratory. Temperature chips were implanted prior to exposure. The studies were approved by University of Pittsburgh's IACUC. Animals were exposed via aerosol in the class-III biosafety cabinet. Plethysmography data was collected to determine dose. Aerosol was calculated by multiplying the all-glass impinger (AGI) (CFU/mL) by the AGI volume (10 mLs) by the aerosol time (1/10 min) by the AGI flow rate (1 min/6 L). The dose was calculated by multiplying the aerosol (CFU/L) by

minute volume (mL/min) by a conversion factor (1L/1000mL) by the duration of the aerosol (10 min). The bronchoalveolar lavage was collected at time of necropsy by inserting 10 mL PBS into the lungs and removing the PBS from the lungs. Dilutions were made and plated on CHA plates.

### **3.3 CELL CULTURE**

The A549 and J774 cell lines were originally obtained from the ATCC. The J774 cells were then cryopreserved in FBS containing 10% DMSO, and stored in a LN2 freezer. The A549 cells were then cryopreserved in a base medium of DMEM-10 containing 10% DMSO, and stored in a LN2 freezer. The cells are thawed by diluting the vial contents with DMEM-10 media containing 1x penicillin and streptomycin, and 10% fetal bovine serum, and ultimately removing the cells from the DMSO containing freezing medium through a series of washes. The cells are centrifuged at 600xg for 5 minutes for each wash step. Then the cells are resuspended in DMEM-10 containing 1x penicillin and streptomycin, and 10% fetal bovine serum and put in a flask. Cells are split every few days when they reach confluency. J774 cells are removed from the flask using a cell scraper. A549 cells are removed from the flask using 2 mL trypsin after 3 washes with PBS.

### **3.4 BACTERIA**

Three *F. tularensis* strains of varying virulence were used in this project. A *F. tularensis* subspecies *novicida* strain (U112), a *F. tularensis* subspecies *holarctica* strain (LVS), and a *F.*

*tularensis* subspecies *tularensis* strain (SCHU S4) were used. These strains are the most commonly used in laboratories to look at intracellular infection by *F. tularensis*. The SCHU S4 and LVS strains are grown for 48 hours before use. The U112 strain is grown for 24 hours before use because it grows at an accelerated rate on CHA compared to LVS and SCHU S4.

### 3.5 INFECTION ASSAY

Two days pre-infection, LVS and SCHU S4 is streaked onto a CHA plate. One-day pre-infection cells are harvested and centrifuged for 5 minutes at 600xg in DMEM-10 with antibiotics. The cells are resuspended in 10-15 mLs of DMEM-10 without antibiotics. The cells are counted using a hemocytometer and concentration is adjusted to 300,000 cells/mL. One mL of cells is put into each well of a 12-well plate. The plates are placed in the incubator overnight at 37 °C and 5% CO<sub>2</sub>. U112 is streaked onto a CHA plate one day pre-infection as well. On the day of infection, a loop full of bacteria is mixed into PBS and read on the microplate reader or spectrophotometer. Once the OD is close to the desired OD (0.08 for the plate reader in the BLS-2 lab and 0.1 for the spectrophotometer in the BSL-3 lab; wavelength: 600), the media is dumped out of the wells and 100 µL of the PBS solution is added to each well. The plates are incubated for 2 hours at 37°C with 5% CO<sub>2</sub>. At the end of the incubation period, the wells are washed 3 times with PBS containing 50 µg/mL of gentamicin. Then 1 mL of media containing 50 µg/mL of gentamicin is added to each well. The plates incubated for 1 hour at 37°C and 5% CO<sub>2</sub>. At the end of the incubation period, the cells are washed with PBS without antibiotics. 0.02-1% SDS is added to the 0 hours post-infection (HPI) wells, while 2 ml of DMEM-10 containing 2 µg/mL of gentamicin is added to the remaining wells. After waiting 10 minutes for the SDS to lyse the

cells, the cell lysate is serially diluted to  $10^{-5}$  and plated on CHA quad plates. The bacterial inoculum is serially diluted as well out to  $10^{-8}$  and plated on CHA quad plates. The plates are placed in the incubator at  $37^{\circ}\text{C}$  and 5%  $\text{CO}_2$ . At the 24, 48 and 72-hour time points the cells are lysed, serially diluted and plated the same way as above. The colonies are counted 48 hours after being plated for LVS and SCHU S4, while the U112 plates are counted 24 hours after being plated. The infection efficiency was calculated by taking the CFU at 0 HPI and dividing it by the inoculum. Doubling was calculated by subtracting the log of 0 HPI multiplied by 3.32 from the log of the other timepoints.

### **3.6 HBE INFECTION ASSAY**

Two days prior to infection, LVS and/or SCHU S4 was streaked onto a CHA plate. The cells were obtained from Mike Myerburg's lab (Division of Pulmonary, Allergy and Critical Care Medicine, University of Pittsburgh, Department of Medicine). The media was removed, wells washed with PBS and antibiotic free media was added. Cells were washed with DTT then PBS three times to remove extracellular debris and mucous. The bacterial inoculum was prepared by taking a sample of the bacteria off of the plates and mixing it into PBS. The inoculum was adjusted using OD. Once the desired OD was reached, 50  $\mu\text{l}$  of the inoculum was added to the top of each well. The plates were incubated at  $37^{\circ}\text{C}$  for 2 hours. The inoculum was removed from the 0 HPI wells. The cells were incubated with 100  $\mu\text{l}$  PBS with 50  $\mu\text{g}/\text{mL}$  gentamicin for an hour. The cells were washed with PBS 3 times. The last wash volume was brought up to 1 mL. Dilutions were made and plated. The cells were then lysed with 0.02% SDS up to a total volume of 1 mL. A pipette tip was used to help lyse the cells. The tip was moved in

circles around the well inserts then in cross motions. Once the cells were lysed, dilutions were made and 50  $\mu$ l were plated on CHA quad plates. The plates were incubated at 37°C for 48-72 hours and the colonies were counted. The cells were lysed at 0 and 24 HPI. See results section for assay development.

### **3.7 CASPASE-3 FLUORESCENT ASSAY IN CELL CULTURES**

This protocol is adopted from the Abcam Caspase 3 Assay Kit manual (ab39383). The infection assay will be performed as described above until the lysing step. The cells will be harvested by adding 100  $\mu$ l trypsin to each well. After the cells detach from the plate, 900  $\mu$ l of DMEM-10 without antibiotics is added. The cells are pelleted by centrifugation at 6000xg for 5 minutes. The cells are washed with PBS, counted and  $1-5 \times 10^6$  cells are pelleted by centrifugation. The pellet is resuspended in 50  $\mu$ L of chilled Cell Lysis Buffer. The solution is incubated on ice for 10 minutes. The samples can be frozen at -80°C at this point. DTT is added to 2X reaction buffer (10 $\mu$ l DTT per mL 2X reaction buffer) immediately before use. 50  $\mu$ L of reaction buffer mix is added to each of the samples. 5  $\mu$ L of the 1 mM DEVD-AFC substrate is then added to each sample. The samples are incubated at 37°C for 1-2 hours. The samples are read on a fluorometer at an excitation of 355 nm and an emission of 520 nm.

### **3.8 CASPASE-3 FLUORESCENT ASSAY IN TISSUES**

Rabbits were serially sacrificed after being infected with SCHU S4. The rabbit tissues were harvested and frozen at -80°C. The frozen tissues were thawed and cut into 0.03-0.05 g pieces. The tissues were homogenized in 1 mL chilled cell lysis buffer. The samples were incubated for 10 minutes. Samples were pelleted by centrifugation at 20000xg for 2-5 minutes. The supernatant was transferred to a clean tube. The samples can be frozen at -80°C at this point. 50 µl of each sample is transferred to a well in a 96-well plate. DTT is added to the 2X reaction buffer immediately before use. 50 µl of the reaction buffer mix is added to each well. 5µl of DEVD-AFC substrate is added to each well. The plate is incubated (protected from light) for 1-2 hours at 37°C. The samples are read on a fluorometer at an excitation of 355 nm and an emission of 520 nm.

### **3.9 CASPASE-1 FLUORESCENT ASSAY IN CELL CULTURES**

This protocol is adopted from the Abcam Caspase 1 Assay Kit manual (ab39412). The infection assay will be performed as described above until the lysing step. The cells will be harvested by adding 100 µl trypsin to each well. After the cells detach from the plate, 900 µl of DMEM-10 without antibiotics is added. The cells are pelleted by centrifugation at 6000xg for 5 minutes. The cells are washed with PBS, counted and  $1-5 \times 10^6$  cells are pelleted by centrifugation. The pellet is resuspended in 50 µL of chilled Cell Lysis Buffer (Abcam). The solution is incubated on ice for 10 minutes. The samples can be frozen at -80°C at this point. DTT (Abcam) is added to 2X reaction buffer (10µl DTT per mL 2X reaction buffer) immediately

before use. 50  $\mu$ L of reaction buffer mix is added to each of the samples. 5  $\mu$ L of the 1 mM YVAD-AFC substrate (Abcam) is then added to each sample. The samples are incubated at 37°C for 1-2 hours (protected from light). The samples are read on a fluorometer at an excitation of 355 nm and an emission of 520 nm.

### **3.10 CASPASE-1 FLUORESCENT ASSAY IN TISSUES**

This protocol is adopted from the Abcam Caspase 1 Assay Kit manual (ab39412). The infection assay will be performed as described above until the lysing step. The cells will be harvested by adding 100  $\mu$ l trypsin to each well. After the cells detach from the plate, 900  $\mu$ l of DMEM-10 without antibiotics is added. The cells are pelleted by centrifugation at 6000xg for 5 minutes. The cells are washed with PBS, counted and  $1-5 \times 10^6$  cells are pelleted by centrifugation. The pellet is resuspended in 50  $\mu$ L of chilled Cell Lysis Buffer (Abcam). The solution is incubated on ice for 10 minutes. The samples can be frozen at -80°C at this point. DTT (Abcam) is added to 2X reaction buffer (10 $\mu$ l DTT per ml 2X reaction buffer) immediately before use. 50  $\mu$ L of reaction buffer mix is added to each of the samples. 5  $\mu$ L of the 1 mM YVAD-AFC substrate (Abcam) is then added to each sample. The samples are incubated at 37°C for 1-2 hours. The samples are read on a fluorometer at an excitation of 355 nm and an emission of 520 nm.

### **3.11 HEMATOXYLIN AND EOSIN STAINING**

The first three steps of this protocol were performed by dipping the slide in xylene for 3 minutes each time. These steps removed the paraffin on the slides. The next four steps were varying percentages of ethanol (100, 100, 95 and 70). These steps were a minute a piece. The next two steps were one-minute wash steps. The next step was the hematoxylin staining step. The slides were placed in hematoxylin for three minutes. There were two thirty second wash steps. The slide was immersed in acid alcohol for thirty-five seconds. There were two thirty second wash steps. The next step was the bluing step with Scott's tap water for thirty seconds. There were two one-minute wash steps. Next was the eosin staining step (2 minutes). The next four steps are the dehydrating steps with the same ethanol used above in reverse order. The last three steps are one-minute xylene steps.

### **3.12 TUNEL ASSAY**

The Invitrogen Click-iT TUNEL Colorimetric IHC Detection Kit was used. First, the cells were deparaffinized by placing slides in xylene twice for five minutes, 1:1 xylene:100% ethanol for five minutes, 100% ethanol for 5 minutes then 3 minutes, 95% ethanol for 3 minutes, 85% ethanol for 3 minutes, 75% ethanol for 3 minutes, 50% ethanol for 3 minutes, 0.85% NaCl for five minutes and then 1X PBS for 5 minutes. Proteinase K (Invitrogen) was added so that the whole tissue was covered. Samples were incubated for 10-20 minutes at room temperature. The slides were washed by immersing in PBS for five minutes. The slides were immersed in fixative solution for five minutes at room temperature. The slides were rinsed with PBS then washed by



immersion in PBS for five minutes twice. The slides were rinsed with deionized water. 100  $\mu$ l of TdT Reaction Buffer (Invitrogen) was added to each slide (covering the whole tissue). The slides were incubated for 10 minutes at 37°C. The TdT Reaction Mixture (Invitrogen) was prepared by adding 558 $\mu$ l TdT Reaction Buffer (Invitrogen), 10 $\mu$ l EdUTP (Invitrogen), and 30 $\mu$ l TdT Enzyme (Invitrogen). The TdT Reaction Buffer (Invitrogen) was removed by blotting with a Kimwipe. 50 $\mu$ l of the TdT Reaction Mixture (Invitrogen) was added to each slide. The slides were incubated for one hour at 37°C. The slides were rinsed with PBS and immersed in 2X SSC for fifteen minutes. The slides were washed twice by immersing them in PBS for five minutes. The slides were immersed in 3% hydrogen peroxide for five minutes at room temperature. The slides were washed twice by immersion in PBS for five minutes. The slides were washed twice with 1X Click-iT TUNEL Colorimetric Wash solution (Invitrogen) for five minutes. The 1X Click-iT TUNEL Reaction Buffer Additive (Invitrogen) working solution was prepared by diluting the solution 1:10 in deionized water. The Click-iT TUNEL Colorimetric Cocktail was prepared by adding 510 $\mu$ l 1X Click-iT Reaction Buffer (Invitrogen), 24 $\mu$ l CuSO<sub>4</sub> (Invitrogen), 6 $\mu$ l Biotin Azide (Invitrogen), and 60 $\mu$ l 1X Click-iT Reaction Buffer Additive working solution. 50  $\mu$ l of the Click-iT TUNEL Colorimetric Reaction Cocktail was added to each slide. The slides were incubated protected from light for 30 minutes at 37°C. The slides were rinsed with PBS then washed twice with the 1X Click-iT TUNEL Colorimetric Wash solution (Invitrogen) for 5 minutes. The slides were rinsed with deionized water then about 200  $\mu$ l of 1X Streptavidin-Peroxidase Conjugate (Invitrogen) was added to each slide. The slides were incubated at room temperature for 30 minutes. The slides were washed three times for 5 minutes with PBS. The slides were rinsed with deionized water and excess water was removed. 5  $\mu$ l of DAB Chromogen (Invitrogen) was added to 95  $\mu$ l DAB substrate buffer for each slide. The 100  $\mu$ l was added to

each slide and incubated for a maximum of 10 minutes at room temperature. The slides were washed thoroughly with deionized water. Slides were counterstained with methyl green. 0.05% methyl green solution was made in sodium acetate. Slides were washed in distilled water after staining. Slides were immersed in methyl green solution for five minutes. The slides were rinsed with distilled water. Next, the slides were dehydrated by immersion in 95% ethanol 10 times. The slides were dipped in 100% ethanol 10 times. That step was repeated. The slides were cleared by immersion in xylene.

### **3.13 SLIDE CUTTING**

Slides were cut on a microtome. Tissue blocks were placed on the microtome. The blade was changed to ensure clean cuts. The blade was pushed up against the block and locked into place. The wheel was rotated to move the block up and down. Sections were cut at 5 microns. As the sections came off in ribbons, the ribbons were carefully placed on top of warm water. The sections of the ribbons were separated by gently poking holes in the wax as it warmed. A clean glass slide was angled in the water under each section and carefully moved upward to “catch” the section on the slide. Slides were placed at an angle to allow water to run off and then incubated overnight at 57°C.

### 3.14 LUNG DIGEST

First, a piece of lung tissue was weighed and placed in a petri dish. The piece was minced with scissors into 1 cm pieces. The lung pieces were placed in a 50 ml conical with 25 ml digestion media. The tubes were placed in a 37°C water bath for 45-60 minutes. After incubation, the pieces were transferred back to the petri dish. The pieces were mashed with a 5 ml syringe plunger and washed with HBSS-Hepes-DNaseI. The tissue was mashed carefully, to prevent it from becoming slimy. The liquid was run through a 70µm cell strainer sitting in a 50 ml conical. The tubes were centrifuged at 600xg for 10 minutes. The supernatant was removed and placed in Oakridge tubes. The Oakridge tubes were centrifuged at 4000xg for 10 minutes to get free bacteria. The pellet was resuspended in 20 ml of PBS, dilutions were made and plated on CHA. The pellet remaining after the supernatant was moved to Oakridge tubes is resuspended in 10 ml of ACK lysing buffer. The ACK mixture was incubated for 5-10 minutes at room temperature. After incubation, the total volume was brought up to 50 ml with PBS. The tubes were centrifuged at 600xg for 10 minutes at 4°C. The supernatant was removed, and the pellet was washed with 30-40 ml of MACs buffer. The tubes were centrifuged at 600 xg for 10 minutes at 4°C. The supernatant was removed, and cells were resuspended in 1 ml of freezing media (90% FBS and 10% DMSO) and frozen at -80°C.

## 4.0 IN VITRO MODEL OF INFECTION

The first aim of this project was to determine whether *F. tularensis* could infect human primary lung epithelial cells at an air-liquid interface and to compare that with conventional *in vitro* infection of A549 cells, a transformed human lung epithelial cell line, and J774 cells, a transformed murine macrophage cell line that is commonly used with *F. tularensis*. Three strains of *F. tularensis* were used: U112, LVS, and SCHU S4. Overall, this aim focuses on the ability of *F. tularensis* to infect and replicate in these cells.

### 4.1.1 Initial Infection Assays

First, the infection assay was performed using J774 cells only. Next, I compared the ability of *F. tularensis* to infect and replicate in A549 cells to that of infection in J774 cells. For the initial assays, J774 (a mouse macrophage cell line) and A549 (a human alveolar epithelial cell line) were infected with one of three strains of *F. tularensis* (U112, LVS, SCHU S4). U112, LVS and SCHU S4 have been used in experiments individually and occasionally two have been compared; however, the goal of this experiment was to demonstrate whether infection and replication in lung epithelium had a role in virulence of the different strains. Although the infections were performed on separate days, the same passage of eukaryotic cell stocks were used for all the assays with a target multiplicity of infection (MOI) of 100. The actual MOIs for

the three infections were slightly higher than the target of 100. The LVS infection had an MOI of 106. The U112 infection had an MOI of 119. The SCHU S4 infection had an MOI of 131 based on the bacterial inoculum that was plated (Table 1). Unfortunately, some time points had cells in a nonquantifiable range. Also, there was no growth at several time points for SCHU S4 and LVS, so the data is not shown.

**Table 1. J774 and A549 Infection.**

Strain	Cell Type	Eukaryotic Cells (log <sub>10</sub> )	MOI	Infection at Time 0 (CFU)	Infection Efficiency (%)
U112	A549	5.58	119	3150	0.0070
U112	J774	5.58	119	2131	0.0047
LVS	A549	5.58	133	200	0.0004
LVS	J774	5.58	133		
SCHU S4	A549	5.58	165	2113	0.0034
SCHU S4	J774	5.58	165	1163	0.0019

J774 and A549 cells were infected with U112, LVS and SCHU S4. The number of cells plated 24 hours pre-infection, MOI calculated by dividing the CFU by the number of cells plated, CFU at time 0 and infection efficiency. The CFU at 0 HPI and infection efficiency are blank for J774 cells infected with LVS because no colonies grew on the 0 HPI CHA plates. Infection efficiency is calculated by dividing the CFU at 0 HPI by the MOI times number of cells (300,000).

Since there were missing time points from the first assay, the assay was performed again with just the J774 cells. Again, the target MOI was 100. However, the MOI for U112 and LVS assays was 70 and the MOI for the SCHU S4 assay was lower at 48 (Table 2). In the previous experiment, there were 380,000 cells/well. In this experiment, there were only 300,000 cells/well. Therefore, there would be less cell-to-cell interaction, which could impact cell-to-cell

infection. There was data for every time point and strain of *F. tularensis* (Figure 1). The U112 and SCHU S4 counts increased at every time point, which was not expected based on published results and previous experiments in the laboratory. Whereas, the LVS counts increased between 0 and 24 HPI, but remained steady through 72 HPI (Figure 1). Typically, the colony counts peak at 24 or 48 HPI and drop at 72 HPI.

**Table 2. J774 Infection Assay.**

Strain	Cell Type	Eukaryotic Cells (log <sub>10</sub> )	MOI	Infection at Time 0 (CFU)	Infection efficiency (%)
U112	J774	5.48	150	967	0.0021
LVS	J774	5.48	100	1717	0.0057
SCHU S4	J774	5.48	103	2750	0.0089

J774 infection assay with U112, LVS and SCHU S4. The number of cells plated 24 pre-infection, MOI, CFU at Time 0, and infection efficiency are shown. Infection efficiency is calculated by dividing the CFU at 0 HPI by the inoculum.

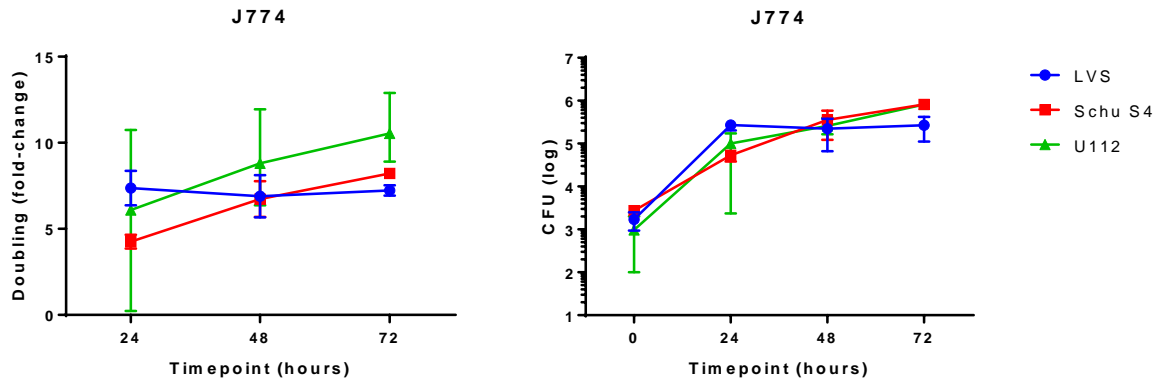


**Figure 1. J774 Infection Assay.**

J774 cells infected with U112, LVS and SCHU S4. Lysate was serially diluted and plated on CHA quad plates. Colonies were counted 48 hours later. Doubling rates at 24, 48 and 72 (left) hours and colony counts at 0, 24, 48 and 72 HPI (right) are shown. Samples were performed in triplicate. Means and ranges are shown.

Next the same assay as above was performed with A549 cells only. The MOIs for this assay were lower than previously at 42, 78 and 20 for U112, LVS and SCHU S4 respectively (Table 3). Again, the U112 counts increased at every time point. Nothing grew for SCHU S4 at 24 HPI, but the counts increased at both 48 and 72 HPI. There was no growth on the plates for the LVS infection at 0, 24 or 72 HPI (Figure 2). This may be a result of not mixing the inoculum well enough before adding it to each well. Also, the lysate may not have been mixed well before making the dilutions or the bacteria could have been lysed as well. During this assay, the supernatant was plated on CHA at the 24 HPI. There was growth on the U112 plate. Therefore, the gentamicin might not have been killing all the extracellular bacteria. Consequently, the results from these three assays cannot be described as intracellular spread from cell-to-cell only. This could be important because cell-to-cell spread could be a way of evading the immune system in the host.

**Table 3. A549 Infection Assay 1.**

Strain	Cell Type	Eukaryotic Cells (log <sub>10</sub> )	MOI	Infection at Time 0 (CFU)	Infection Efficiency (%)
U112	A549	5.58	42	540	0.0034
LVS	A549	5.58	78		
SCHU S4	A549	5.58	20	47	0.0006

A549 cells were infected with U112, LVS and SCHU S4. The number of cells plated 24 hours pre-infection, MOI, CFU at 0 HPI and infection efficiency are shown below. Infection efficiency is calculated by dividing the CFU at 0 HPI by the inoculum.

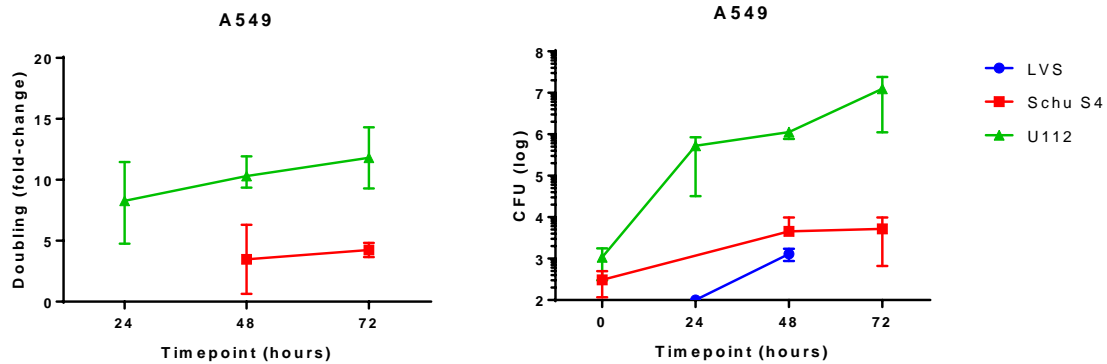


**Figure 2. A549 Infection Assay 1.**

A549 cells infected with U112, LVS and SCHU S4. Lysate was serially diluted and plated on CHA quad plates. Colonies were counted 48 hours later. Doubling rates at 24, 48 and 72 (left) hours and colony counts at 0, 24, 48 and 72 HPI (right) are shown. Samples were performed in triplicate. Means and ranges are shown.

#### 4.1.2 Lung Epithelial Cell Infection

Since there were issues with getting results at each timepoint, I decided to focus on infecting the A549 cell line with SCHU S4 and LVS, but not U112. The infection assay was performed as previously described with new gentamicin. Eight infection assays were performed at once. Two of the infection assays were used to collect data on colony counts and doubling rates. The remaining assays were used to collect samples for the caspase-1 and caspase-3 assays. To improve the assay protocol, during the lysing step the pipet tip was used to break up the A549 layer. The tip was moved in concentric circles around the wells and then in a cross motion to improve the lysing process. This was especially necessary at the 48 and 72 HPI timepoints because the epithelial cells were more confluent at these timepoints.



**Table 4. A549 Infection Assay 2.**

Strain	Cell Type	Eukaryotic Cells (log <sub>10</sub> )	MOI	Infection at Time 0 (CFU)	Infection Efficiency (%)
SCHU S4	A549	5.48	61.7	3050	0.0165
LVS	A549	5.48	68.3	250	0.0012

A549 cells were infected with LVS and SCHU S4. The number of cells plated 24 hours pre-infection, MOI, CFU at 0 HPI and infection efficiency are shown below. Infection efficiency is calculated by dividing the CFU at 0 HPI by the inoculum.

Although the OD predicted the MOI would be 100, the MOIs ended up being 62 and 68 bacteria per eukaryotic cell. This assay had exactly 300,000 cells in each well. At timepoint zero, the average number of LVS that were able to infect the cells was 93. While, over 2500 SCHU S4 bacteria were able to infect the cells. The infection efficiencies for both bacteria are extremely low at below one percent (Table 4). Both the LVS and the SCHU S4 followed the predicted growth rates and doubling. SCHU S4 peaked at 24 HPI and LVS peaked at 48 HPI (Figure 3).

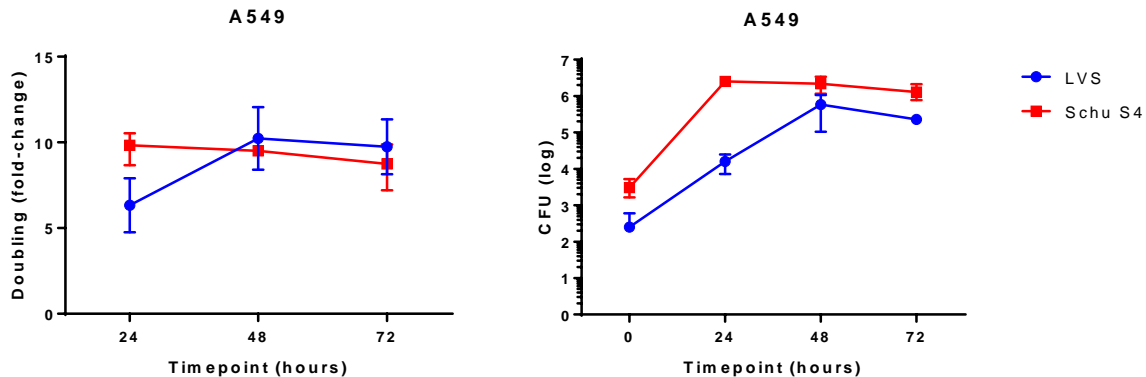


**Figure 3. A549 Infection Assay 2.**

A549 cells were infected with LVS and SCHU S4. Lysate was serially diluted and plated on CHA quad plates. Colonies were counted 48 hours later. Doubling rates at 24, 48 and 72 (left) hours and colony counts at 0, 24, 48 and 72 HPI (right) are shown. Only two wells of LVS had growth at 0 HPI, therefore LVS 0 HPI is the average of two wells and all LVS doubling rate are an average of two wells. All SCHU S4 data is the average of three wells. Means and ranges are shown.

The assay was repeated for reproducibility. The MOIs were higher for LVS and SCHU S4 compared to the previous assay (Table 5). However, both strains had lower CFU at 0 HPI. The growth rates for SCHU S4 peaked at 48 HPI as compared to 24 HPI. The doubling rates from both experiments follow the same pattern. LVS peaked at 48 HPI in both infection assays; however, it had high replication rates in the second infection assay. Overall, these data suggest that LVS and SCHU S4 have similar growth and doubling rates in A549 cells (Figure 4). However, SCHU S4 typically had a higher capacity to infect than LVS initially. The differences seen in the infection assays could be due to the bacteria used. While the initial loopfuls came from the same aliquot, the bacteria do not always recover the same from being thawed. Alternatively, it could just be experimental variation.

**Table 5. A549 Infection Assay 3.**

Strain	Cell Type	Eukaryotic Cells (log <sub>10</sub> )	MOI	Infection at Time 0 (CFU)	Infection efficiency (%)
SCHU S4	A549	5.48	66.7	467	0.0023
LVS	A549	5.48	86.7	123	0.0005

A549 cells were infected with LVS and SCHU S4. The number of cells plated 24 hours pre-infection, MOI, CFU at 0 HPI and infection efficiency are shown below. Infection efficiency is calculated by dividing the CFU at 0 HPI by the inoculum.

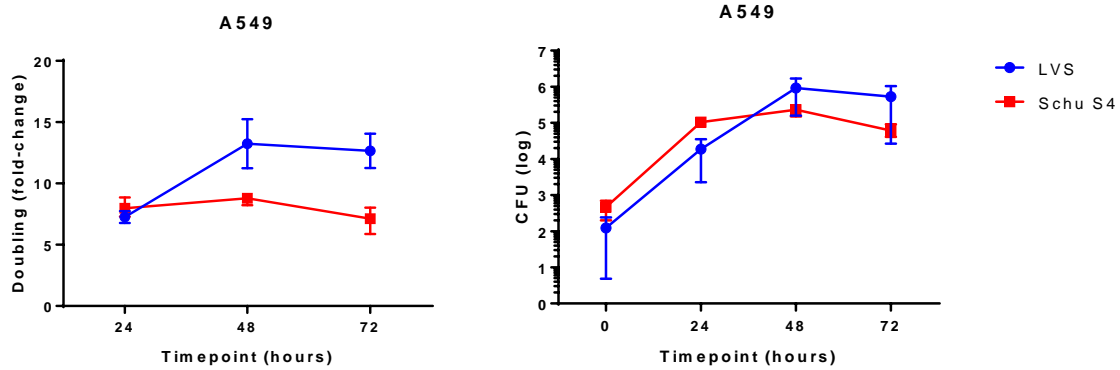


**Figure 4. A549 Infection Assay 3.**

A549 cells infected with LVS and SCHU S4. Lysate was serially diluted and plated on CHA quad plates. Colonies were counted 48 hours later. Doubling rates at 24, 48 and 72 (left) hours and colony counts at 0, 24, 48 and 72 HPI (right) are shown. Samples were performed in triplicate. Means and ranges are shown.

A549 cells were infected with SCHU S4 as previously described. Cells were lysed and the caspase levels were assessed using fluorescence. The plates were supposed to be read at 400/505nm; however, the machine was unable to read at these wavelengths. The plates were read at 355/520nm. There were no significant differences in the fluorescence between timepoint and uninfected controls (Figure 5).

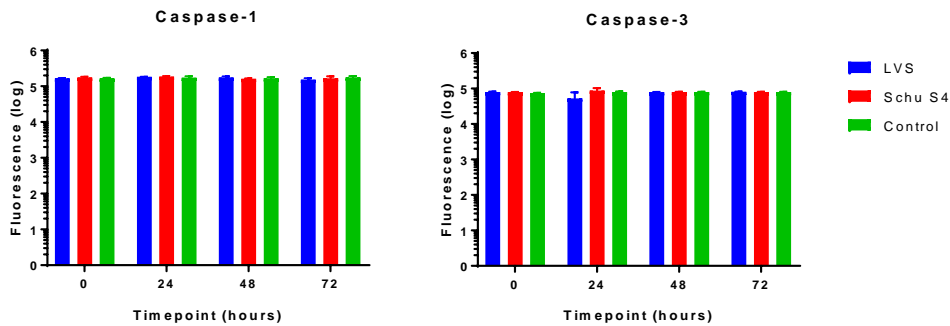


**Figure 5. A549 Caspase-1 and Caspase-3.**

A549 cells were infected with SCHU S4. Cells were lysed and caspase levels were assessed. No difference in fluorescence levels was seen. Samples were performed in triplicate. Means and ranges are shown.

### 4.1.3 Human Primary Lung Infection

The protocol used in the previously mentioned experiments was used to develop an infection assay for a 3D culture of human primary lung epithelium. These cultures are designed to mimic the structure of the epithelium in the human lung. These cells develop cilia, produce mucous and are polarized. The human bronchial epithelium was provided by Mike Myerburg's lab (Division of Pulmonary, Allergy and Critical Care Medicine, University of Pittsburgh, Department of Medicine). The cells were obtained from his lab, washed to remove antibiotics and antibiotic free media was added. The first infection assays were performed with LVS only. The bacterial inoculum was created by adding a loopful of bacteria to PBS. The target MOI for the first assay was 10. 10  $\mu$ l of bacterial inoculum was added to each well (Table 6). The cells were incubated for three hours at 30°C and 5% CO<sub>2</sub>. At the end of the incubation, PBS was added to the top. The liquid was removed, diluted and plated. The cells were then washed several times with PBS. The cells were lysed using 0.02% SDS. However, this would not lyse the cells. Sterile water was also used to try to lyse cells and it did not work as well. The 0.02% SDS was used again in combination with pipetting up and down which eventually lysed the cells. The cell lysate was diluted and plated. The media from the bottom of the wells was also diluted and plated. The idea was to see where the bacteria was: still on top of the cells, in the cells or through the cells. There was no growth on almost all the plates. There was growth for 1/6 of the top layer sets of plates (Table 6). From this infection assay, it was concluded that the MOI, infection time and amount of bacterial inoculum plated may influence the assay. The cells used for this assay came from a donor with silicosis. This could have influenced the cells susceptibility to *F. tularensis*.

**Table 6. HBE Infection Assay 1.**

MOI	Amount Plated	Incubation	0 HPI Counts	24 HPI Counts	Cell ID	Disease
19.5	10 µl	2 Hours	All 0/0 except one top	All 0/0	191	Silicosis

HBE cells from a donor with silicosis were infected with LVS at an MOI of 19.5. 10 µl of inoculum were plated onto the cells. There was no LVS in the cell lysate and media at 0 HPI. One out of six wells of HBE cells had LVS growth in the inoculum wash at 0 HPI. There was no LVS in the cell lysate, media, or inoculum wash at 24 HPI.

To address some of the possible issues from the first assay, another infection assay was performed. Different MOIs, incubation times and inoculum plated were tested (Tables 7 and 8). Cells from a healthy donor were used for this assay. This time only the cell lysate was diluted and plated. The cells were also lysed differently this time. The 0.02% SDS is added to each well and the pipette tip is used to scrape the cells of the film. This action also helps lyse the cells. Again, there was no growth on any of the plates (Table 8). Therefore, the question became: can *Francisella* even infect primary human lung epithelium?

**Table 7. HBE Assay 2 Plate Setup.**

MOI:100	MOI: 100	MOI: 100	MOI:100	MOI: 10	MOI: 10
100 µl	100 µl	50 µl	50 µl	50 µl	50 µl
2 Hours	2 Hours	2 Hours	2 Hours	2 Hours	2 Hours
MOI:100	MOI: 100	MOI: 100	MOI:100	MOI: 10	MOI: 10
100 µl	100 µl	50 µl	50 µl	50 µl	50 µl
3 Hours	3 Hours	3 Hours	3 Hours	3 Hours	3 Hours

HBE cells were infected with 50-100 µl of LVS inoculum at target MOI of 100 or 10. The cells were incubated with the inoculum from 2 to 3 hours.

**Table 8. HBE Infection Assay 2.**

Amount Plated	MOI	Cell ID	Disease	0 HPI Counts
100 $\mu$ l	160	195	None	All 0/0
50 $\mu$ l	322.5	195	None	All 0/0
50 $\mu$ l	27.25	195	None	All 0/0

HBE cells from a healthy donor were infected with LVS at MOIs from 27.25-322.5. Inoculum was plated in 50-100  $\mu$ l amounts. There was no growth in the cell lysate at 24 HPI.

To address this question the assay was repeated using 50  $\mu$ l and MOI of 10 (Table 9). Again, the cells were from a healthy donor. However, only a 24-hour timepoint was plated. Also, the cells were infected with SCHU S4 and LVS to determine if there is a strain difference in infection. There was growth on both the LVS and SCHU S4 plates (Figure 6). This suggests that *F. tularensis* can infect primary human bronchial epithelium.

**Table 9. HBE Infection Assay 3.**

Strain	Amount Plated	MOI	Cell ID	Disease
LVS	50 $\mu$ l	7	190	None
SCHU S4	50 $\mu$ l	12.25	190	None

HBE cells from a healthy donor were infected with two strains of *F. tularensis*: LVS and SCHU S4 at MOIs from 7-12.25. The inoculum was plated in 50  $\mu$ l amounts.

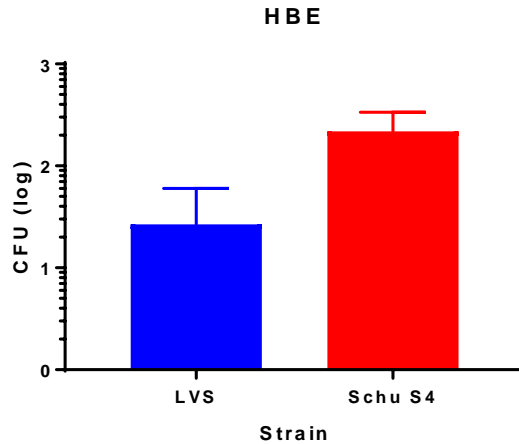


**Figure 6. LVS and SCHU S4 colony counts in HBE cell lysate 24 hours post-infection.**

HBE cells from a healthy donor were infected with LVS and SCHU S4. There was no growth at 0 HPI. The CFU/ml lysate are shown. Samples were performed in triplicate. Means and ranges are shown.

The assay was repeated to confirm results; however, there was inconsistency in the results. The cells used for this assay were from a donor with silicosis. The MOIs were similar to the MOIs in the previous assay (Table 10). There was growth at 24 HPI (Figure 7), but there was no growth at 0, 48, 72, or 96 HPI (Table 10). It was suggested that using PBS could be impacting the bacteria's ability to survive in the inoculum.

**Table 10. HBE Infection Assay 4.**

Strain	MOI	Cell ID	Disease	0 HPI Counts	48 HPI Counts	72 HPI Counts	96 HPI Counts
LVS	8	191	Silicosis	0/0	0/0	0/0	0/0
SCHU S4	12.25	191	Silicosis	0/0	0/0	0/0	0/0

HBE cells from a donor with silicosis were infected with LVS and SCHU S4 at MOIs from 8-12.25. There was no growth on the 0 HPI and 48 HPI plates. The PBS used for 72 and 96 HPI dilutions was contaminated, but there was no growth from the lysate.

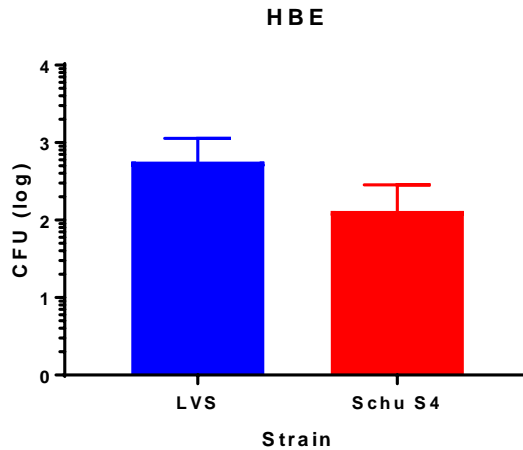


**Figure 7. HBE Infection Assay 4.**

HBE cells from a donor with silicosis were infected with LVS and SCHU S4. There was growth at 24 HPI for both the LVS and SCHU S4 infected cells. Samples were performed in triplicate. Means and ranges are shown.

Another assay was performed using BHI and PBS for the inoculum. *Francisella* grows well in BHI, so if PBS was the problem, the results should have been more consistent. The MOIs were slightly lower than previous assays. The cells used for this assay were from a healthy donor (Table 11). However, again the results were inconsistent (Figure 8). The colony counts ranged from 2-60 within the replicate wells. There could be several explanations for the inconsistent results. First, cells from different donors were used for each assay. While the cells were from different donors, the results should still be consistent when compared to that same patient and this was not true. Therefore, that explanation seemed unlikely. Second, some of the CHA plates used in the last assay were dry and bumpy by the time the plates were counted. However, there was growth on some of the dry and bumpy plates. Finally, the assay protocol did not use antibiotics to kill the extracellular bacteria before lysing. Therefore, some extracellular bacteria may have been trapped in the cilia or mucous causing the higher colony counts. This seemed to be the most likely cause of inconsistency. To address this issue, several steps were added to the assay protocol. A DTT rinse was added to remove the mucous layer before infection to allow the



bacteria to access the cells easier. Also, a thirty-minute incubation with PBS with 50 µg/ml gentamicin was added. The wells were washed three times after to remove all the gentamicin. The last washing step was plated to confirm that all of the extracellular bacteria were killed with the gentamicin.

**Table 11. HBE Infection Assay 5.**

Strain	Media	MOI	Cell ID	Disease
SCHU S4	PBS	7.25	190	None
SCHU S4	BHI	7.75	190	None

HBE cells from a healthy donor were infected with SCHU S4 at MOIs from 7.25-7.75. The inoculum was prepared in PBS and BHI.

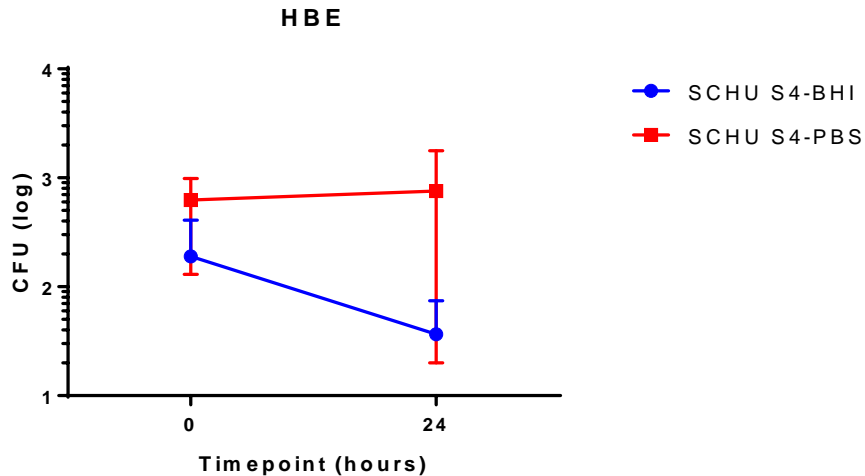


**Figure 8. HBE Infection Assay 5.**

There was growth in the HBE lysate at 0 and 24 HPI. The counts were inconsistent within the replicate wells. Samples were performed in triplicate. Means and ranges are shown.

Cells from a donor with bronchopulmonary dysplasia and another donor with scleroderma and pulmonary arterial hypertension were used for this assay. The MOIs were higher than previous assays (Table 12). The additions to the protocol did not kill or remove all

the extracellular bacteria in the wells. All the last wash plates had colonies (Table 12). There was growth at 0 and 24 HPI (Figure 9). The quantity of intracellular bacteria could not be quantified due to the presence of bacteria in the last wash.

**Table 12. HBE Infection Assay 6.**

MOI	Cell ID	Disease	0 HPI Wash	24 HPI Wash
15	197	Bronchopulmonary dysplasia	Positive	Positive
15	199	Scleroderma/Pulmonary arterial hypertension	Positive	Positive

HBE cells from a donor with bronchopulmonary dysplasia and another with scleroderma and pulmonary arterial hypertension were infected with SCHU S4 at a MOI of 15. All last washes contained SCHU S4.

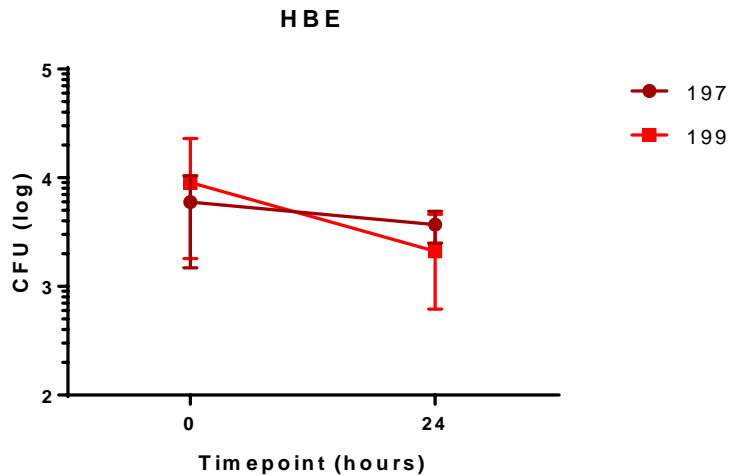


**Figure 9. HBE Infection Assay 6.**

Lysate from both HBE cell lines contained SCHU S4 at 0 HPI and 24 HPI. Samples were performed in triplicate. Means and ranges are shown.

The gentamicin step is an hour for the A549 cells, so the gentamicin incubation time for the HBE cells was increased to an hour. Also, 900  $\mu$ l of PBS was added to the 100  $\mu$ l of last wash, dilutions were made and plated. The last wash CFU were subtracted from the lysate CFU to predict the number of intracellular bacteria. This assay was performed with cells from a donor

with bronchopulmonary dysplasia and another donor with scleroderma and pulmonary arterial hypertension. The MOIs were lower than the previous assay (Table 13). There was growth in the last wash and lysate; however, the growth in the lysate was higher than the last wash (Figure 10). I concluded that *F. tularensis* can infect HBE cells.

**Table 13. HBE Infection Assay 7.**

MOI	Cell ID	Disease
6.75	197	Bronchopulmonary dysplasia
6.75	199	Scleroderma/Pulmonary arterial hypertension

HBE cells from a donor with bronchopulmonary dysplasia and another with scleroderma and pulmonary arterial hypertension were infected with SCHU S4 at a MOI of 6.75.

The assay was performed again for reproducibility with the cells from the donor with bronchopulmonary dysplasia. The MOI was higher than the previous assay, which may explain the higher wash and lysate counts (Table 14). Again, there was growth in the lysate and last wash at 0 and 24 HPI (Figure 11).

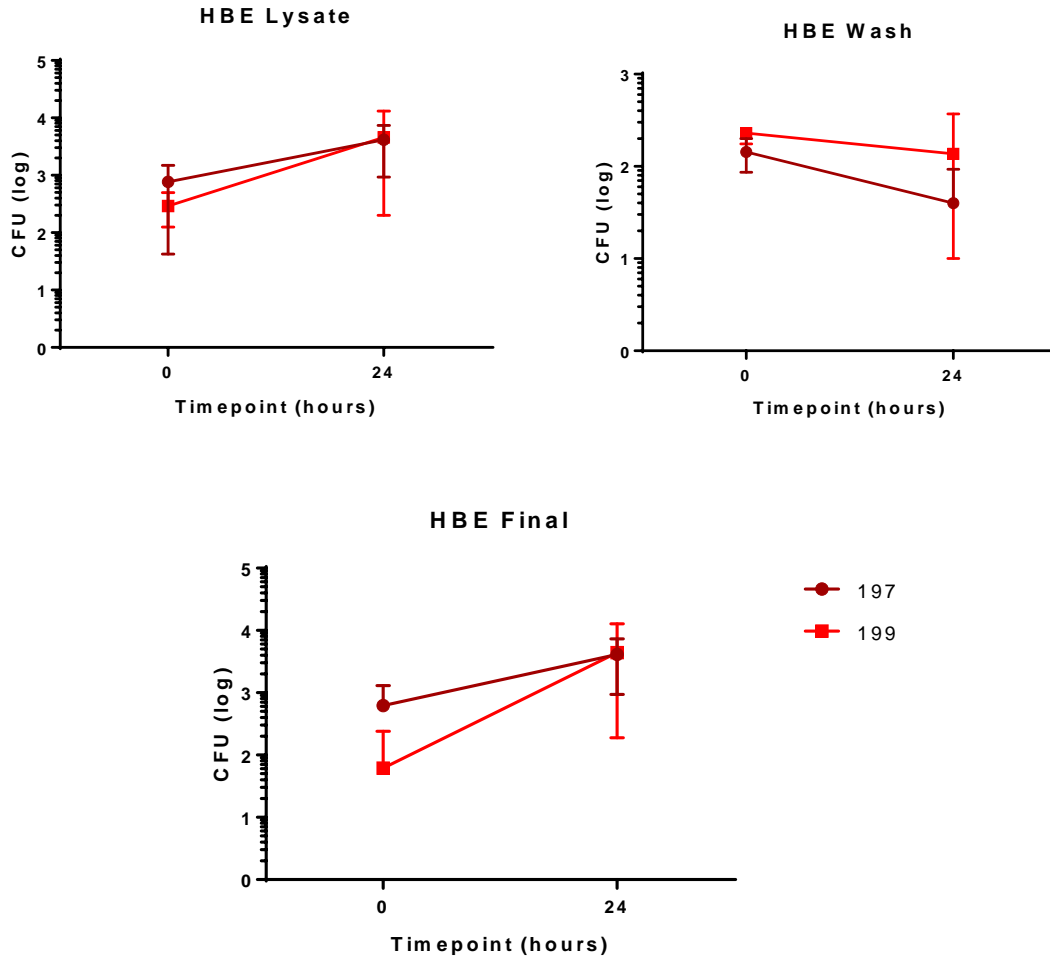


**Figure 10. HBE Infection Assay 7.**

Colony counts from last wash (top right) were subtracted from colony counts from cell lysate (top left). The results are shown (bottom). There are more colonies in the lysate than in the wash proving that SCHU S4 is infecting the HBE cells. Samples were performed in triplicate. Means and ranges are shown.

**Table 14. HBE Infection Assay 8.**

MOI	Cell ID	Disease
15	197	Bronchopulmonary dysplasia

HBE cells from a donor with bronchopulmonary dysplasia were infected with SCHU S4 at a MOI of 15.

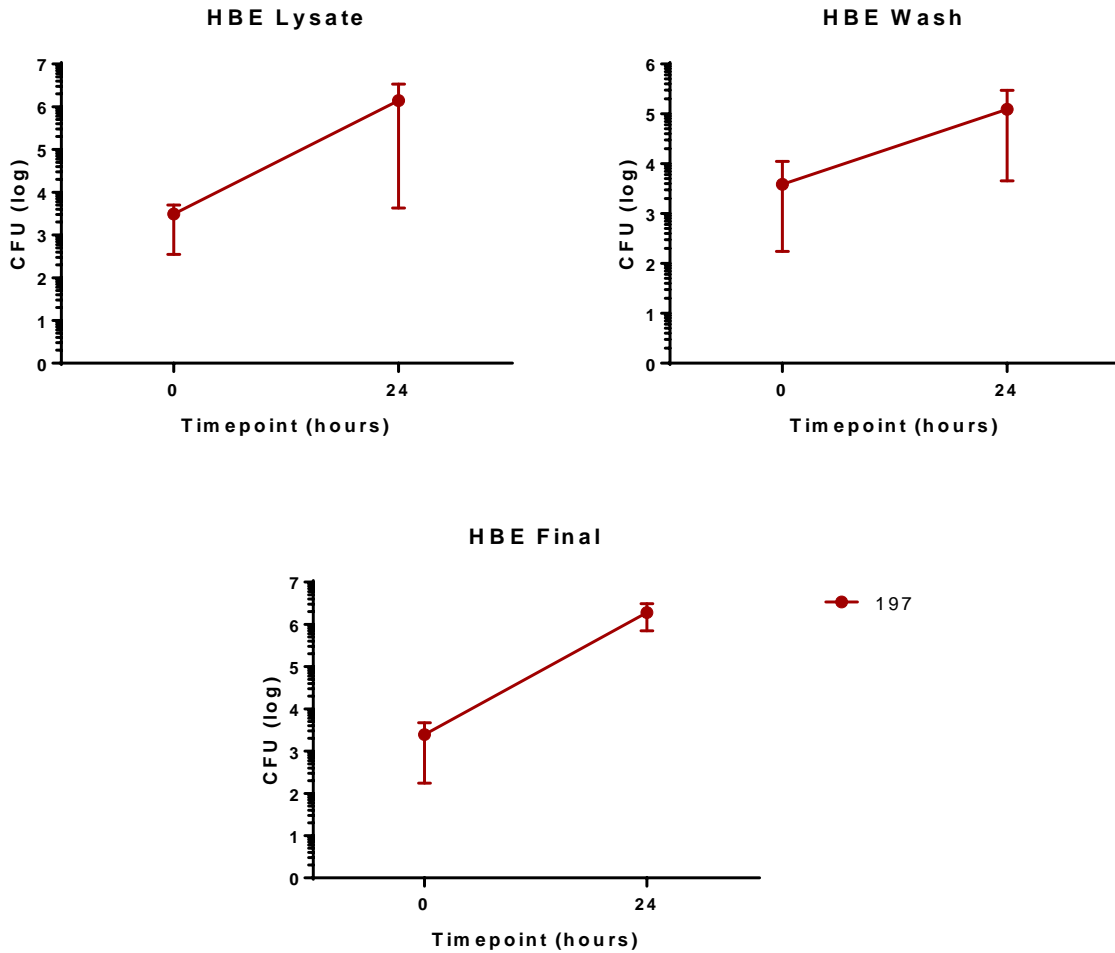


**Figure 11. HBE Infection Assay 8.**

Colony counts from last wash (top right) were subtracted from colony counts from cell lysate (top left). The results are shown (bottom). There are more colonies in the lysate than in the wash proving that SCHU S4 is infecting the HBE cells. Samples were performed in triplicate. Means and ranges are shown.

## 4.2 PATHOGENESIS IN RABBIT LUNGS

Rabbit tissues from a previous study were used. There were 12 rabbits in this study. Three rabbits were not infected before they were sacrificed. The remaining rabbits were serially sacrificed one, two and three days post exposure. There were three rabbits sacrificed at each time

point. At the time of sacrifice, the bronchoalveolar lavage was taken to determine presence of *Francisella*. The lungs from eight out of the nine infected rabbits' lungs were digested. Some of the lung digest was serially diluted and plated on CHA plates to determine the presence of bacteria. The remaining tissues were harvest and frozen at -80°C. The lower left lung sections were homogenized later. Homogenate was plated to determine presence of bacteria. Also, the homogenate was lysed for caspase-1 and caspase-3 assays. There were three uninfected rabbits in this study; however, they were sacrificed differently than the infected rabbits. Also, there were positive colony counts for all three in the lower left lung of all three uninfected rabbits. Therefore, the controls were not used for the caspase and TUNEL staining. There were no other uninfected rabbit tissues to use as controls. More uninfected rabbits will have to be sacrificed for controls in the future.

All infected rabbits received similar doses during the aerosol. The rabbits sacrificed three days post-exposure had slightly higher doses than the other rabbits. Bronchoalveolar lavage (BAL) was taken at time of necropsy. The BAL increased with each day post-exposure. The lung digest and homogenate colony counts peaked at day two post-exposure (Figure 12). Typically, unvaccinated rabbits develop fevers around day three post-exposure. The rabbits in this study developed fevers around day two or three post-exposure (Figure 12).

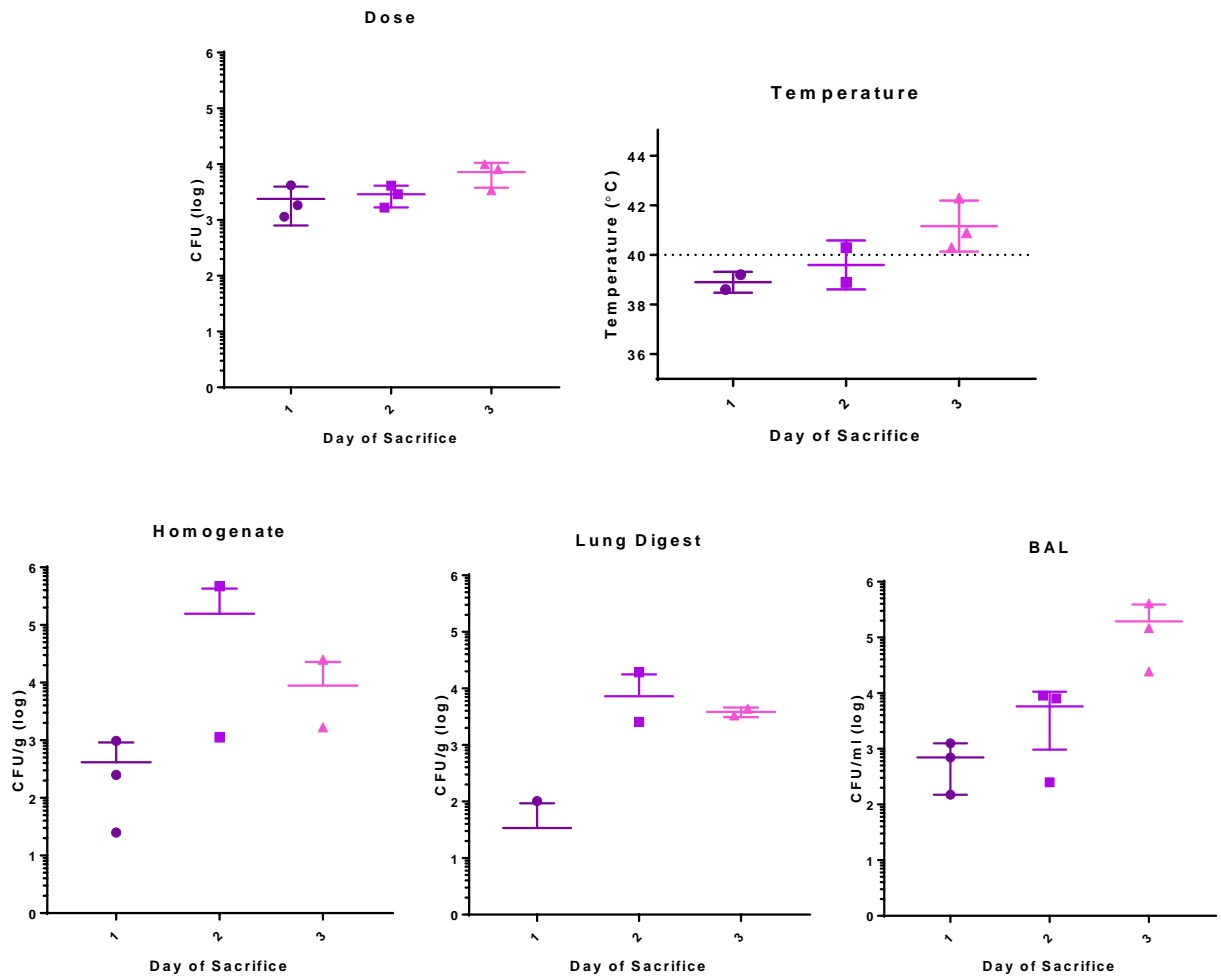


**Figure 12. *Francisella tularensis* in Rabbit Lung Tissue.**

Lung tissue from rabbits sacrificed one, two and three days post-exposure was digested and titers were plated. Frozen lower left lung tissue was homogenized and titers were plated. Both homogenate and lung digest CFU/g peaked two days post-exposure. BALs were performed on rabbits during the necropsy. The CFU in the BAL increased with each day post-exposure. Mean and ranges are shown.

#### 4.2.1 Caspase Assays

For the caspase assays the frozen tissues were thawed, weighed and homogenized in chilled cell lysis buffer. The samples were frozen and the assay was performed later. The plates

were supposed to be read at excitation/emission: 400/505 nm; however, the plate reader was unable to read at these wavelengths. Therefore, the first plates were read at 355/520 nm. There were no significant caspase differences in the infected and uninfected rabbit tissues. There were slightly higher caspase-1 levels in the rabbits sacrificed one day post-exposure. There were slightly higher caspase-3 levels in the rabbits sacrificed one day and three days post-exposure (Figure 13).

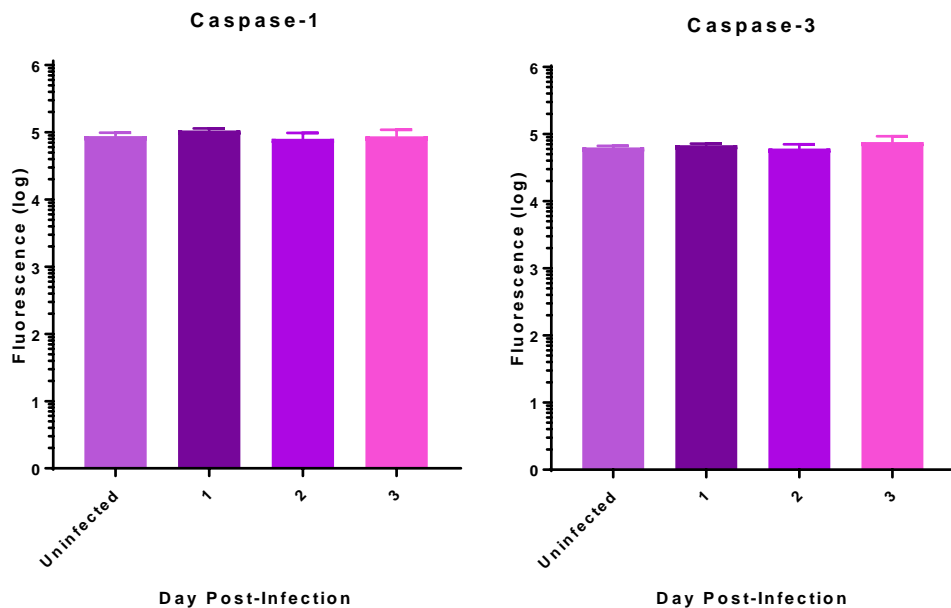


**Figure 13. Rabbit Caspase Staining.**

The presence of caspase-1 and caspase-3 in lower left lung homogenate from rabbits sacrificed one, two and three days post-exposure. There does not appear to be any difference in the caspase levels in the infected and uninfected rabbits.

#### 4.2.2 Lung Slides

Sections of the lungs of the rabbits were also paraffin-embedded and cut onto slides. Each rabbit tissue had a slide stained with H&E and a slide stained with TUNEL. Two of the



rabbits sacrificed one day post-exposure had healthy, uninflamed lungs. However, one showed evidence of some inflammation and hemorrhaging (Figure 14). One rabbit sacrificed two days post-exposure had a high amount of inflammation and hemorrhaging. The other rabbit showed no evidence of inflammation or hemorrhaging. Also, one rabbit sacrificed three days post-exposure had a high amount of inflammation and hemorrhaging, while the other appeared to have healthy lungs (Figure 14).

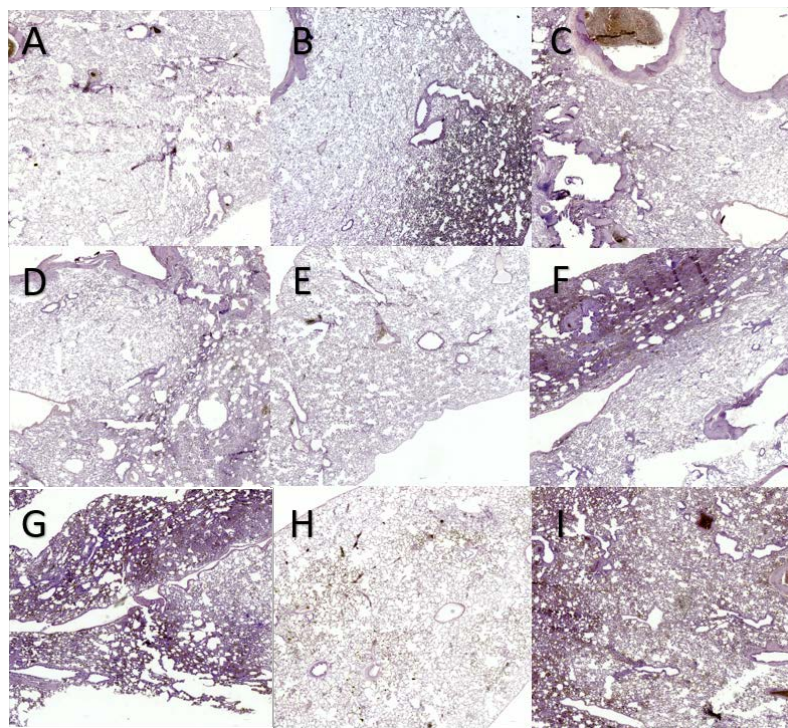


**Figure 14. Inflammation in the lower left lung of rabbits sacrificed one to three days post-exposure to SCHU-S4.**

Lower left lung tissue from rabbits sacrificed one (A-D), two (E-G) and three (H-I) days post-exposure were stained with hematoxylin and eosin. Images were taken at 10x magnification. Inflammation and hemorrhaging increases each day post-exposure.

The slides were TUNEL stained as well. There is a small amount of DNA fragmentation in one of the rabbits sacrificed one day post-exposure. There is more DNA fragmentation in the rabbits sacrificed two days post-exposure. There is a higher amount of DNA fragmentation,

suggesting apoptosis, in the rabbits sacrificed three days post-exposure than the two days prior (Figure 15).

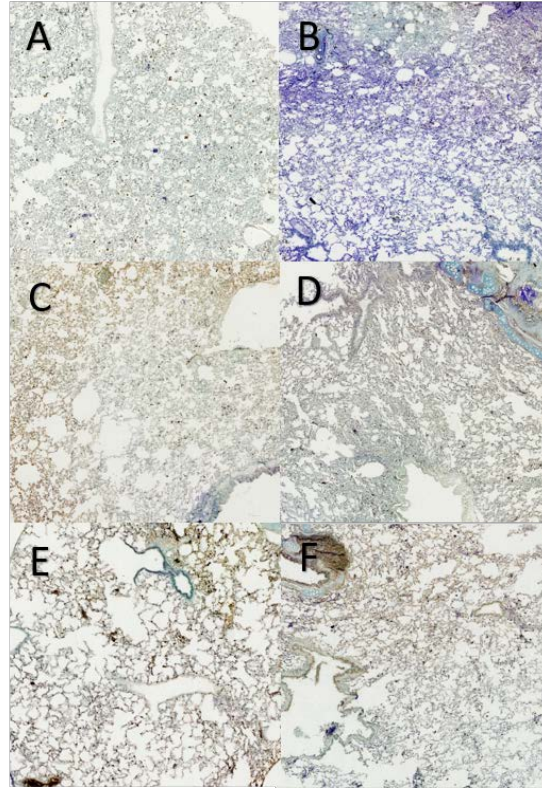


**Figure 15. DNA fragmentation in the lower left lung of rabbits sacrificed one to three days post-exposure to SCHU-S4.**

Lower left lung from rabbits sacrificed one (A-B), two (C-D) and three (E-F) days post-exposure were TUNEL stained. Images were taken at 10x magnification. The DNA fragmentation levels appear to increase each day post-exposure. Although, the DNA fragmentation is present the level of DNA fragmentation is not high. There is some background seen on the slides (C).

To confirm these results, slides from the upper right lung were cut. Also, lung tissue from rabbits sacrificed four and five days post-exposure were cut. The inflammation varied throughout each tissue sample, but it increased each day post-exposure (Figure 16). Specifically, the tissue from the rabbits sacrificed four days post-exposure showed extremely high levels of inflammation. There were almost no alveolar regions throughout the tissue. Edema can be seen in the tissues from the rabbits sacrificed five days post-exposure (Figure 18).

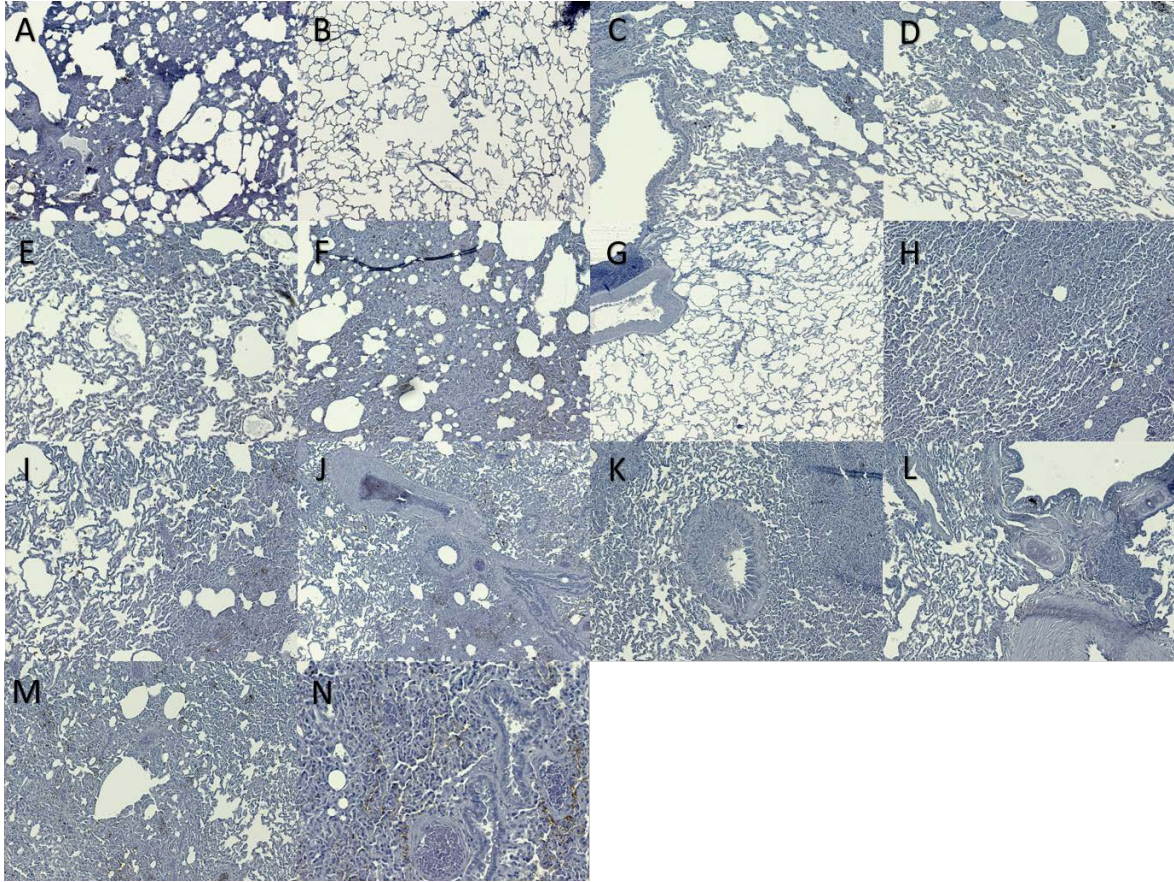


**Figure 16. Inflammation in the upper right lung rabbits sacrificed one to three days post-exposure to SCHU-S4.**

Upper right lung tissue from rabbits sacrificed one (A-D), two (E-H) and three (I-N) days post-exposure were stained with hematoxylin and eosin. Images are in pairs from the same rabbit to show varying levels of inflammation within the sections. Images were taken at 10x magnification. The most inflammation and hemorrhaging were seen in the rabbits sacrificed three days post-exposure.

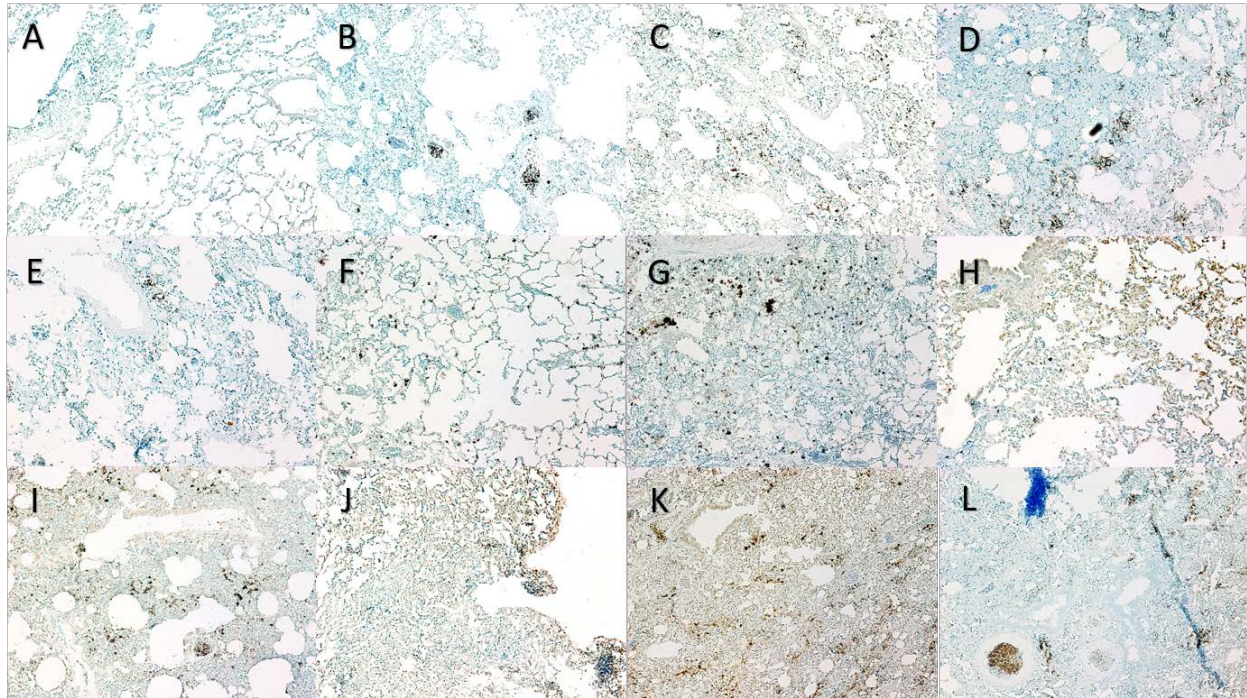


**Figure 17. DNA fragmentation in upper right lung of rabbits sacrificed one to three days post-exposure to SCHU-S4.**

Upper right lung tissue from rabbits sacrificed one (A-C), two (D-H) and three (I-L) days post-exposure were TUNEL stained. Images were taken at 10x magnification. The DNA fragmentation levels appear to increase each day post-exposure. Although, the DNA fragmentation is present the level of DNA fragmentation is not high. There was high background on most slides and control slides (not shown).

The slides were also TUNEL stained. There appears to be increasing amounts of DNA fragmentation in the tissues (Figure 17). There were high levels of background on the control slide and several of the other slides. The background makes it difficult to definitively say there is TUNEL positive staining. The highest levels of TUNEL positive staining were seen in one rabbit sacrificed four days post-exposure and one sacrificed five days post-exposure (Figure 19). There were nodules in some of the rabbit tissues. These nodules stained TUNEL positive in the rabbit lung tissue from the rabbits sacrificed four days post-exposure (Figure 19).

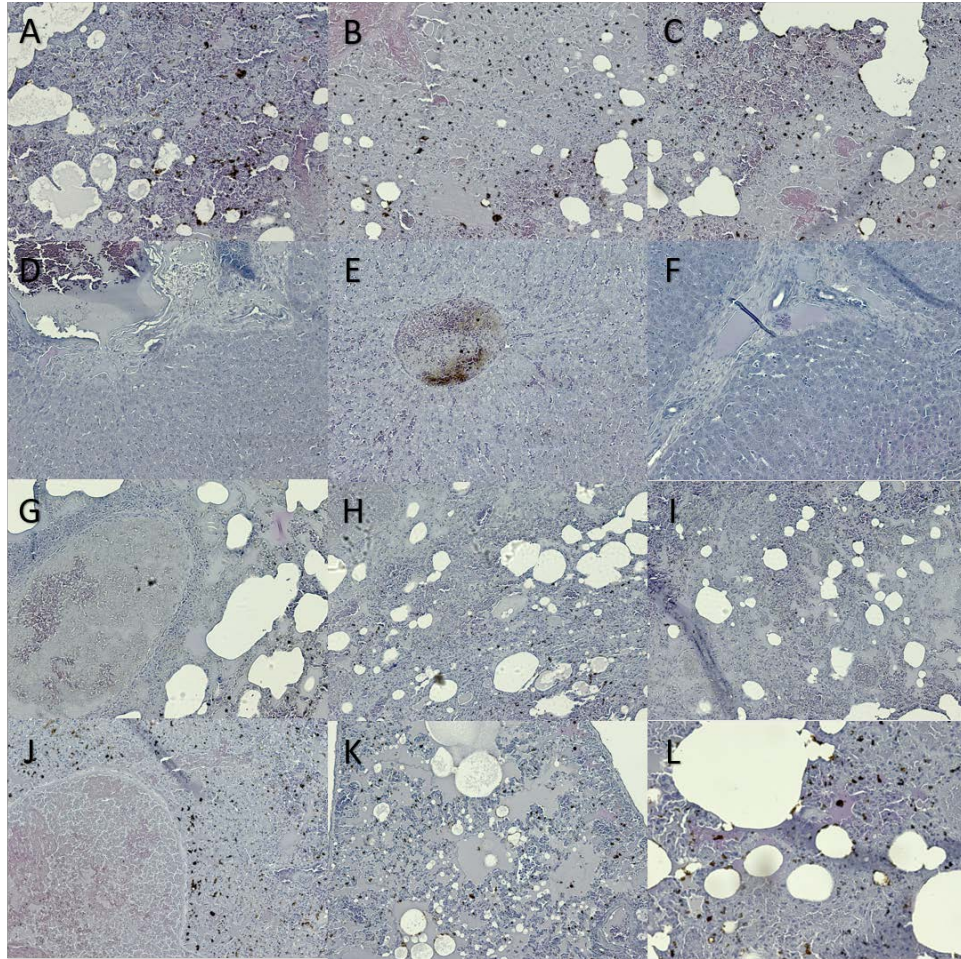


**Figure 18. Inflammation in the lung of rabbits sacrificed four and five days post-exposure to SCHU S4.**

Lung tissue from rabbits sacrificed four (A-F) and five (G-L) days post-exposure were stained with hematoxylin and eosin. Images are in triplicate from the same rabbit. Images were taken at 10x magnification. The most inflammation was seen in the rabbits sacrificed four days post-exposure (D-F).

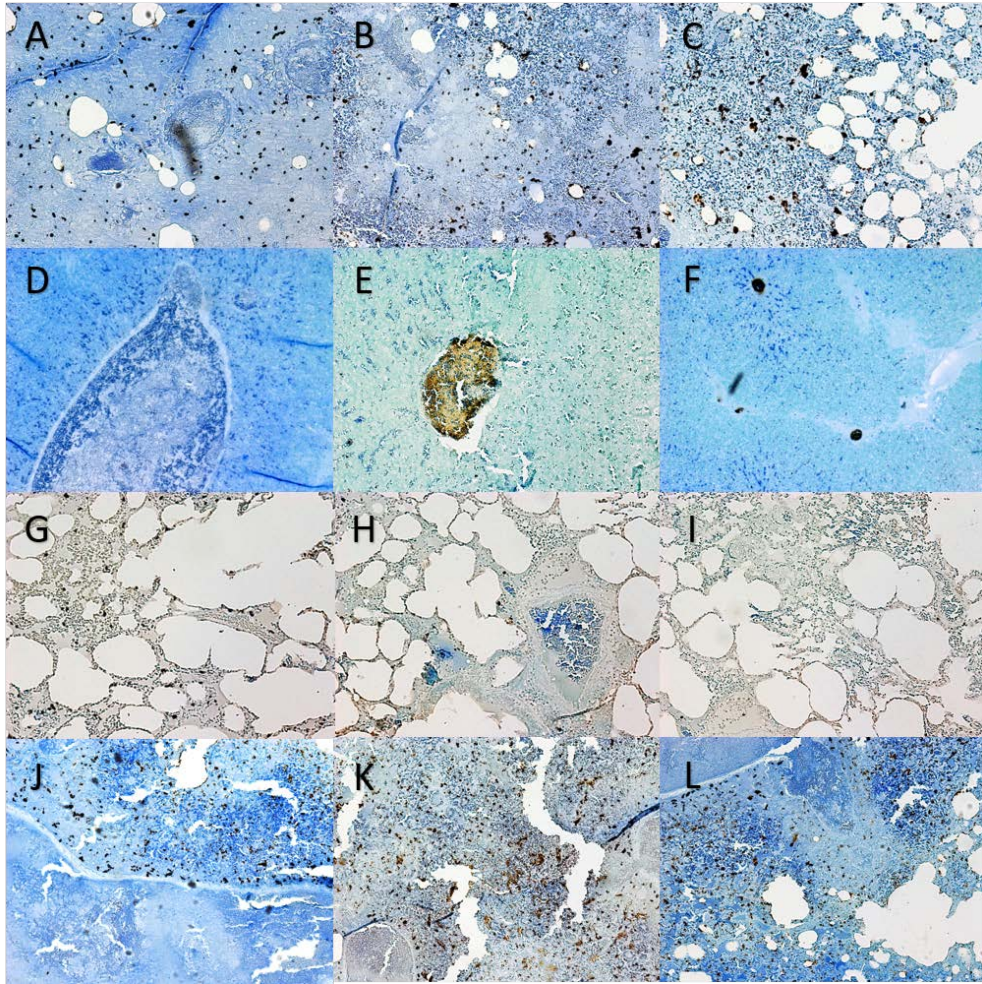


**Figure 19. DNA fragmentation in lung tissue from rabbits sacrificed four and five days post-exposure to SCHU S4.**

Lung tissue from rabbits sacrificed four (A-F) and five (G-L) days post-exposure were TUNEL stained. Images were taken at 10x magnification except image F. F was taken at 5x magnification. The DNA fragmentation levels vary between rabbits. The levels are higher in one rabbits sacrificed four days post-exposure (A-C) and five days post-exposure (J-L) than the rabbits sacrificed one to three days post-exposure (shown previously).

Overall, it appears that cell death and inflammation increased from one to four days post-exposure to SCHU S4. The inflammation was slightly decreased in the rabbits sacrificed five days post-exposure. The hemorrhaging increased from one to three days post-exposure in the lung tissues. In the future, the results will be compared to new uninfected controls that were sacrificed the same way and do not have bacteria in the lungs.

## 5.0 DISCUSSION

Previous groups have studied the cell types infected by *Francisella* in the lungs of mice. They found that U112, LVS and SCHU S4 strains of *Francisella* were able to infect alveolar macrophages, CD11b<sup>high</sup> macrophages, CD11b<sup>low/mid</sup> dendritic cells, CD11b<sup>high</sup> dendritic cells, monocytes, neutrophils and alveolar type II epithelial cells. Not surprisingly, they found that one day post-infection that alveolar macrophages composed most infected cells for all three strains. Both the macrophages and alveolar type II epithelial cells had higher numbers of infected cells at one day post-infection when compared to three days post-infection [24]. The bacteria must peak between 24 and 48 HPI. Therefore, I expected to see similar results with our *in vitro* work. I found the growth rates peaked at 24 or 48 hours post-infection, indicating my *in vitro* work is consistent with the published *in vivo* studies. *F. tularensis* disseminates quickly through the body; therefore, by day three the bacteria are likely disseminating throughout the body and no longer needs to replicate at high levels in the epithelial cells.

Based on those prior studies I expected that *F. tularensis* could infect both macrophages and lung epithelial cells. While macrophages are typically the focus of tularemia research, lung epithelial cells could also be important. There are far more epithelial cells along the surface of the lungs for bacteria to interact with than macrophages. Type II epithelial cells exchange gas and maintain a fluid balance. Their proximity to endothelial cells could aid in the dissemination of bacteria [3]. We found that *F. tularensis* can replicate at similar rates within A549 and J774

cells. Although, we found that the bacteria can infect more J774 cells initially than A549 cells. Due to the phagocytic nature of J774 cells this was an expected result. In our study, we found that the infection efficiency was lower than one percent. Hall and associates found that 0.2% of A549 cells were infected after six hours of infection. In comparison the Tc-1 cell line, a mouse lung epithelial cell line, had as high as 17% infected cells. They also found that both the Tc-1 and A549 cell lines had less infected cells than the J774A.1 cell line [12]. Also, one group found that 0.05%-0.1% of the inoculum had successfully infected Hep-2 cells, human bronchial epithelial cells and A549 cells after four hours of infection [19]. Even though our infection efficiencies were lower than these, our infection time was half or a third of these previous study infection times. Ultimately, these data together suggest that *F. tularensis* can infect both macrophages and lung epithelial cells at low rates initially. However, once the *F. tularensis* infected either cell type, it can replicate and infect other cells.

Hall et al. found that *Francisella* localizes to the alveolar regions of the lungs of infected mice one to seven days post-exposure to LVS. They saw very few bacteria in the apical surfaces of the bronchial epithelial cells. They also did not see any replication of bacteria with bronchial epithelial cells [12]. However, Lindemann et al. found that LVS was able to infect human bronchial epithelial cells. I wanted to infect human primary bronchial epithelial (HBE) cells to see if *F. tularensis* truly can infect human bronchial epithelial cells [19]. Also, the primary HBE cells more closely resemble the human lungs. Our preliminary data suggests that *F. tularensis* can infect HBE cells. However, *F. tularensis* is unable to infect the cells after two hours as seen in the A549 experiments. It appears that *F. tularensis* infects HBE cells at a slower rate than A549 cells, since the HBE twenty-four-hour post-infection counts are similar to the two-hour post-infection counts of the A549 cells. Future experiments need to be done to confirm these



results and to characterize the infection in these cells. Ultimately, this infection assay might be useful bridging the gap between the A549 experiment results and the disease in humans.

Currently, it is unclear which type of cell death is induced by *Francisella* infection. Lai et al. observed pro-caspase 9 and 3 cleavage when they challenged J774 cells with LVS. Also, they observed cytochrome c release and degradation of poly-ADP-ribose polymerase and therefore; they concluded that *Francisella* was inducing apoptosis. Other studies found that procaspase-1 was not necessary to induce cell death. Mice deficient in caspase-1 showed similar pathological responses to infection as the wild-type mice. Supporting the idea that the damage caused by cell death is not due to caspase-1 induced cell death. Also, the spleens of these mice stained positively for fragmented DNA and expressed activated caspase-3 supporting the observation that *Francisella* is causing apoptotic cell death in these animals. However, caspase-3 activation, fragmented DNA, necrosis and bacterial dissemination were greater in mice infected with *F. tularensis* isolate KU49 than LVS [25]. Isolate KU49 is more virulent than LVS; therefore, if the damage is caused by apoptotic cell death, then the higher levels of caspase-3 activation, fragmented DNA, necrosis and bacterial dissemination are expected in mice infected with the KU49 isolate.

In contrast, other studies have shown pro-caspase-1 activation in mouse bone marrow derived macrophages after infection with LVS or U112 [25]. Studies with virulent strains of *F. tularensis* have shown low levels of caspase-1 activation [26]. To escape the phagolysosomes, the *Francisella* virulence factor iglC is required. The transcription of virulence factors iglC, pdpD and pdpA is regulated by mglA. MglA and pdpA are required to induce macrophage death. One group found that macrophages from caspase-1 deficient mice were highly resistant to cell death. Also, macrophages from these mice were resistant to *F. tularensis*-induced death when

infected with *mg1A* and *pdpA* mutants. Therefore, *F. tularensis*-induced cell death must be dependent on bacteria replicating in the cytosol and caspase-1 activation. Similarly, apoptosis-associated speck-like protein containing CARD (ASC) deficient macrophages were resistant to cell death induced by *F. tularensis*. ASC is an inflammasome adapter protein. Caspase-1 induced cell death seems to be a host defense against *Francisella* infection [27]. I hypothesized that both caspase-1 and caspase-3 are induced during *Francisella* infection. Based on the previous studies, it appears that pyroptosis is triggered to remove the bacteria from the cytosol where it replicates; however, it does not appear that this is successful in preventing severe disease. Whereas, apoptosis may be part of the pathogenesis of *Francisella*. Tissue damage during infection may be due to *Francisella* inducing apoptosis, since apoptosis is a form of cell death that does not trigger an immune response. Therefore, I expected to see positive caspase-1 and caspase-3 results in my fluorescent assays. Also, I expected to see positive TUNEL staining and caspase-1 staining in the sections from infected rabbit lungs. Unfortunately, I did not see any differences in the fluorescent assays. This could have been due to the inability to read at the correct wavelength, errors in the performing the assay or many other reasons. Ultimately, this experiment will need to be repeated with A549 and HBE cells. My TUNEL stained slides appear to be positive. There is a small amount of positive staining in the rabbit sacrificed one day post-exposure. One rabbit that was sacrificed two days post-exposure had a high amount of positive staining. The other had a medium amount. Both the rabbits sacrificed three days post-exposure had a high amount of positive staining. It appears that cell death increases each day post-exposure; therefore, *F. tularensis* infection is inducing cell death. However, these results do not signify the type of cell death or the cause of the cell death.

Based on previous studies, I expected to see and observed inflammation in the lungs of rabbits euthanized two and three-days post-infection. One group studied forty-two hares that were found dead due to *Francisella*. The researchers found that there was mild or no inflammation in the liver, spleen and bone marrow of these hares. Necrosis and lesions were found on organs throughout many of the hares' bodies. *Francisella* was found in the cytoplasm of several cells types in the muscle of the hares [28]. However, there is no data on the day-post infection that these hares died or how they were infected. Another group infected F344 rats with aerosolized SCHU S4. At the time of death, typically four to five days post-infection, the rats have high bacterial counts in the lungs, liver and spleen. These rats had developed lung, liver and spleen inflammation and severe sepsis. The inflammation was observed in these organs at three days post-infection and increased through day seven post-infection [29]. Hares, rabbits and rats are not the only animals to develop lung inflammation post-infection with *Francisella*. Mice infected with LVS showed inflammation in the lungs six days post-infection [30]. Also, African green monkeys infected with SCHU S4 had hemorrhaging, lesions, edema and congestion in the lungs seven to eleven days post-infection [31]. I did see inflammation in the lower left lungs of the rabbits sacrificed on days two and three post-infection. Previously the activation of apoptosis by *F. tularensis* was mentioned; however, this seems on the contrary of the inflammation seen in the rabbit lungs. The inflammation could be from the immune system triggering pyroptosis to prevent *F. tularensis* from replicating in the cytosol. Cytokines are released during pyroptosis that cause inflammation at the site. Only several of the rabbits in our study developed inflammation in the lower left lung; however, typically the rabbits develop fevers three to four days post-infection. If I looked at tissues from later times points, it is likely that I would see

widespread inflammation. Future experiments will focus on different sections of the lung, other organs and later timepoints.

The doses were similar for all our rabbits in this study; however, the rabbits sacrificed on day three post-infection had slightly higher doses. The bacteria levels in the BALs were highest in the rabbits sacrificed three days post-infection. Since the doses were slightly higher for these rabbits and the bacteria has had longer to replicate and spread, this is expected. The lung digest CFU and homogenate CFU peak two days post-infection. This is somewhat unexpected since the rabbits do not develop fever until three days post-infection. I would expect the CFU to peak on day three or four. However, if pyroptosis is occurring between day two and three, it could explain the higher BAL and the lower tissue counts. Also, *F. tularensis* disseminates throughout the body, so it may use the epithelial cells proximity to enter the circulatory system by day three.

Overall, I think that lung epithelial cells do play an important role in *F. tularensis* pathogenesis. I think the proximity to the circulatory system aids in the dissemination of the bacteria. If we could prevent *F. tularensis* from infecting epithelial cells, maybe the infection could be prevented. Even though it does infect other cell types, if it cannot infect the epithelium, it may not be able to infect enough cells to start a productive infection. Future experimental interests include evaluating the caspase levels in A549 and HBE cells, further evaluating caspase and TUNEL staining in rabbit tissues, evaluating the metabolic impacts of *Francisella* infection on HBE cells and cytokine analysis.

## BIBLIOGRAPHY

1. WHO guidelines on tularemia: epidemic and pandemic alert and responses. 2007, World Health Organization Press: Geneva, Switzerland.
2. Stundick, M.V., et al., *Animal models for Francisella tularensis and Burkholderia species: scientific and regulatory gaps toward approval of antibiotics under the FDA Animal Rule*. Vet Pathol, 2013. **50**(5): p. 877-92.
3. Craven, R.R., et al., *Francisella tularensis invasion of lung epithelial cells*. Infect Immun, 2008. **76**(7): p. 2833-42.
4. Chong, A. and J. Celli, *The francisella intracellular life cycle: toward molecular mechanisms of intracellular survival and proliferation*. Front Microbiol, 2010. **1**: p. 138.
5. Reed, D.S., et al., *Pneumonic tularemia in rabbits resembles the human disease as illustrated by radiographic and hematological changes after infection*. PLoS One, 2011. **6**(9): p. e24654.
6. Kingry, L.C. and J.M. Petersen, *Comparative review of Francisella tularensis and Francisella novicida*. Front Cell Infect Microbiol, 2014. **4**: p. 35.
7. El-Etr, S.H., et al., *Francisella tularensis type A strains cause the rapid encystment of Acanthamoeba castellanii and survive in amoebal cysts for three weeks postinfection*. Appl Environ Microbiol, 2009. **75**(23): p. 7488-500.
8. Cross, A.S., F.M. Calia, and R. Edelman, *From rabbits to humans: the contributions of Dr. Theodore E. Woodward to tularemia research*. Clin Infect Dis, 2007. **45 Suppl 1**: p. S61-7.
9. Parnavitana, C., et al., *Temporal cytokine profiling of Francisella tularensis-infected human peripheral blood mononuclear cells*. J Microbiol Immunol Infect, 2008. **41**(3): p. 192-9.
10. Gillette, D.D., et al., *Virulent Type A Francisella tularensis actively suppresses cytokine responses in human monocytes*. Front Cell Infect Microbiol, 2014. **4**: p. 45.
11. ATTC. J774A.1. Available from: <https://www.atcc.org/Products/All/TIB-67.aspx>.
12. Hall, J.D., et al., *Francisella tularensis replicates within alveolar type II epithelial cells in vitro and in vivo following inhalation*. Infect Immun, 2007. **75**(2): p. 1034-9.
13. Chalabaev, S., et al., *Sensitivity of Francisella tularensis to ultrapure water and deoxycholate: implications for bacterial intracellular growth assay in macrophages*. J Microbiol Methods, 2011. **85**(3): p. 230-2.
14. Holicka, M., et al., *J774 macrophage-like cell line cytokine and chemokine patterns are modulated by Francisella tularensis LVS strain infection*. Folia Microbiol (Praha), 2010. **55**(2): p. 191-200.

15. Broms, J.E., L. Meyer, and A. Sjostedt, *A mutagenesis-based approach identifies amino acids in the N-terminal part of Francisella tularensis IglE that critically control Type VI system-mediated secretion*. *Virulence*, 2017. **8**(6): p. 821-847.
16. ATTC. A549. Available from: <https://www.atcc.org/Products/All/CCL-185.aspx>.
17. Bradburne, C.E., et al., *Temporal transcriptional response during infection of type II alveolar epithelial cells with Francisella tularensis live vaccine strain (LVS) supports a general host suppression and bacterial uptake by macropinocytosis*. *J Biol Chem*, 2013. **288**(15): p. 10780-91.
18. David, J., N.M. Sayer, and M. Sarkar-Tyson, *The use of a three-dimensional cell culture model to investigate host-pathogen interactions of Francisella tularensis in human lung epithelial cells*. *Microbes Infect*, 2014. **16**(9): p. 735-45.
19. Lindemann, S.R., et al., *An in vitro model system used to study adherence and invasion of Francisella tularensis live vaccine strain in nonphagocytic cells*. *Infect Immun*, 2007. **75**(6): p. 3178-82.
20. Carterson, A.J., et al., *A549 lung epithelial cells grown as three-dimensional aggregates: alternative tissue culture model for Pseudomonas aeruginosa pathogenesis*. *Infect Immun*, 2005. **73**(2): p. 1129-40.
21. Brennan Molly, A. and T. Cookson Brad, *Salmonella induces macrophage death by caspase-1-dependent necrosis*. *Molecular Microbiology*, 2002. **38**(1): p. 31-40.
22. Aachoui, Y., et al., *Inflammasome-mediated pyroptotic and apoptotic cell death, and defense against infection*. *Curr Opin Microbiol*, 2013. **16**(3): p. 319-26.
23. Murphy, K.M., et al., *Janeway's immunobiology*. 2017, New York; London: GS, Garland Science, Taylor & Francis Group.
24. Hall, J.D., et al., *Infected-host-cell repertoire and cellular response in the lung following inhalation of Francisella tularensis Schu S4, LVS, or U112*. *Infect Immun*, 2008. **76**(12): p. 5843-52.
25. Wickstrum, J.R., et al., *Francisella tularensis induces extensive caspase-3 activation and apoptotic cell death in the tissues of infected mice*. *Infect Immun*, 2009. **77**(11): p. 4827-36.
26. Hagar, J.A. and E.A. Miao, *Detection of cytosolic bacteria by inflammatory caspases*. *Curr Opin Microbiol*, 2014. **17**: p. 61-6.
27. Mariathasan, S., et al., *Innate immunity against Francisella tularensis is dependent on the ASC/caspase-1 axis*. *J Exp Med*, 2005. **202**(8): p. 1043-9.
28. Hestvik, G., et al., *Francisella tularensis in muscle from diseased hares - a risk factor for humans?* *Epidemiol Infect*, 2017. **145**(16): p. 3449-3454.
29. Hutt, J.A., et al., *The Natural History of Pneumonic Tularemia in Female Fischer 344 Rats after Inhalational Exposure to Aerosolized Francisella tularensis Subspecies tularensis Strain SCHU S4*. *Am J Pathol*, 2017. **187**(2): p. 252-267.
30. Periasamy, S., et al., *Inflammasome-Independent NLRP3 Restriction of a Protective Early Neutrophil Response to Pulmonary Tularemia*. *PLoS Pathog*, 2016. **12**(12): p. e1006059.
31. Twenhafel, N.A., D.A. Alves, and B.K. Purcell, *Pathology of inhalational Francisella tularensis spp. tularensis SCHU S4 infection in African green monkeys (Chlorocebus aethiops)*. *Vet Pathol*, 2009. **46**(4): p. 698-706.